University of Crete, Department of Biology

Institute of Molecular Biology and Biotechnology, FORTH

Molecular Biology, Biomedicine MSc program

Master thesis:

Developing novel tools to characterize *Notch*-triggered malignancy in the central nervous system of *Drosophila melanogaster*

Author:

Gerasimos Anagnostopoulos

Heraklion, 2017

Developing novel tools to characterize *Notch*-triggered malignancy in the central nervous system of *D. melanogaster*.

A Thesis Submitted to

the Department of Biology, University of Crete

Gerasimos Anagnostopoulos

October 2017

Thesis Committee:

Professor Christos Delidakis (UoC, IMBB-FORTH)

Professor Joseph Papamatheakis (UoC, IMBB-FORTH)

Dr. Iannis Talianidis (IMBB-FORTH)

Table of contents:

List of figures:

Summary:

During larval neurogenesis of the fruitfly *Drosophila melanogaster*, Notch signaling contributes to cell-fate decisions in the neuroblast lineage (Artavanis-Tsakonas et al., 1995; Kopan and Ilagan, 2009). However, in case of Notch aberrant activity, a hyperplastic central nervous system of neoplastic transition capacity may arise (Zacharioudaki *et al.*, 2012; Zacharioudaki *et al.*, 2016; Magadi *et al.*, in preparation). We focus on the contribution of Notch signaling in generating malignant tumor phenotype. To address the neoplastic transition, we have utilized the "tissue allograft" method (Gateff, 1994; Rossi and Gonzalez, 2015) in order to transplant *Notch*-derived and *HES*-derived hyperplastic brain lobes into healthy hosts. In the future, we plan to perform transcriptome analysis of the *Notch*-triggered outgrown tumor including its temporal dynamics. We also aim to estimate the extent (if any) upon which *Notch*-derived tumors provoke tumor cell infiltration within healthy tissues and metastases development.

Finally, we have developed a novel genetic scheme in order to address whether the Notch hyperactivity that initiates the tumor outgrowth is still necessary to sustain tumor propagation. To address this hypothesis, we have generated a new transgenic *D. melanogaster* line carrying the *UAS-FRT-Notch$^{\Delta E}$-p2A-DsRed-FRT-nlsEGFP* (*U-NPDG*) transgene. When crossed to a neuroblast-lineage-specific *Gal4*-expressing line, *U-NPDG* transgenic flies have been shown to induce central nervous system hyperplasia during larval neurogenesis.

Abbreviations:

b-HLH	Basic-Helix loop Helix
CDS	Coding sequence
CNS	Central Nervous System
E(spl)	Enhancer of split
FRT	FLP Recombination Target
GMC	Ganglion Mother Cell
HES	*Hairy E(Espl)*
HEY	Hairy Enhancer of split
hsp70	Heat shock promoter 70
LB	Luria Bertani broth
NB	Neuroblast
NICD	Notch intracellular domain
nls	Nuclear Localization Signal
PCR	Polymerase Chain Reaction
rpm	Revolutions per minute
TDC	Tyrosine Decarboxylase (octopamin pathway)
TF	Transcription factor
UAS	Upstream Activating Sequence
U-NPDG	*UAS-FRT-Notch$^{\Delta E}$-2A-DsRed-FRT-nlsEGFP* transgene
VNC	Ventral nerve cord
WRPW	Trp-Arg-Pro-Trp motif
ΔE	Truncated Notch derivative missing most of its extracellular domain

1. Introduction.

1.1. *Drosophila melanogaster* model organism.

1.1.1. Basic features.

The fruit fly *Drosophila melanogaster* as a model has first come to light during 19th century by J.W. Meigen (1833). It has contributed to studies of genetics, inheritance, development, behavior, learning, and aging, among others. This is thanks to its numerous advantages such as ease and inexpensiveness in culturing under laboratory conditions, short life cycle, large numbers of externally laid embryos, high efficiency in genetic modifications and transgenic development. The most essential advantage of *Drosophila melanogaster*, according to Seymour Benzer, is "the enormous store of accumulated knowledge concerning the organism itself" (Benzer, 1967). One of the most significant obstacles to overcome was the sequencing of its entire genome (Adams *et al.*, 2000) which was calculated to be 139 Mb in size that carries approximately 16,000 putative coding regions within four well-marked chromosomes. Moreover, once the simplicity of generating transgenic flies had been comprehensively established (Rubin and Spradling, 1982; O'Connor and Chia, 1993; Handler and Harrel, 1999; Fish *et al.*, 2007), numerous *D. melanogaster* transformants were developed. Thus, various types of transgenes were constructed and transformed within recipient *D. melanogaster* lines. For instance, transgenes were developed in order to activate or inhibit the expression of individual coding regions of interest (in a cell/ tissue-specific manner or throughout the organism). Moreover, taking advantage of the RNA interference technology (Carthew, 2001), knockdown of individual genes of interest in *D. melanogaster* cells was feasible. The introduction of several fluorescent marker proteins (e.g. green fluorescent protein, GFP) contributed to the tissue, cellular or/ and sub-cellular monitoring of proteins of interest *in vivo*. Marker proteins' expression was specific (i) following the pattern of specific genes or (ii) fused in frame with the gene of interest (Tweedie *et al.*, 2009; Matthews *et al.*, 2005).

Extensive studies on the developmental program of the fruit fly model organism have significantly contributed to our knowledge on molecular pathways' crosstalk that regulates stem cell activity in all animals (Pearson *et al.*, 2009). The

development of the *D. melanogaster* is characterized by a fine-regulated spatiotemporal gene expression network. During embryogenesis, cells tend to divide and, given the right stimulus, undergo differentiation towards a specific cell type. Such differentiation process is tightly regulated so as to give rise to complex tissues, avoiding uncontrolled cell division that may lead to pathological phenotypes.

1.1.2. Life cycle.

Drosophila melanogaster is a holometabolous insect displaying a four-stage life cycle that includes fertilized egg, larva, pupa, and adult fly (imago). After fertilization, the eggs are laid and half-buried in the food substrate with their respiratory filaments protruding into the air for gas exchange. The egg hatches after 22–24 hours (at 25°C) and the first instar larva (L1) emerges. The larva constantly consumes water and nutrients from the food substrate and, as a result, it grows in size over five days (second and third instar larval stages) until it undergoes pupation. The pupa is stationary, with its early stages being yellowish-white and later stages get progressively darker. During pupation (3-4 days), the larva gets metamorphosed acquiring the imago's structures and, finally, the imago emerges from the pupal case (eclosion). During metamorphosis, a significant amount of the larval structures get histolysed, while a distinct number of larval organs remains preserved (e.g. nervous system, malpighian tubules, gonads). Most of the adult structures form anew from two cellular sets: the imaginal discs and histoblasts.

An eclosed adult male gets sexually active within hours of emerging, while the female lacks ripe eggs for two days after eclosion. The *D. melanogaster* mating individuals may live for more than 10 weeks. The fertilization is internal, and the sperm is stored within the female's body in the seminal receptacle and the paired spermathecae. A female individual reaches the peak of its egg production between 4th and 7th day after eclosing (50-100 eggs per day).

1.2. *Drosophila melanogaster* central nervous system overview.

The *Drosophila melanogaster* central nervous system (CNS) derives from stem-cell-like progenitors defined as neural stem cells or neuroblasts (NBs). NB contributes to the CNS's fine-orchestrated development from embryonic stages till adulthood (medulla cortex neurogenesis). It divides in an asymmetric manner and, as a result, it gives rise to two distinct cells; one keeping its neuroblast stemness while,

the other (called ganglion mother cell, GMC) acquiring an immature differentiating "identity". The GMC is capable of dividing only once, producing terminally differentiated daughter cells (neurons, glia). Two division modes have been described for larval NBs: a Type I neuroblast generates a GMC, while a Type II neuroblast generates an intermediate neural precursor (INP). INP undergoes division once more, giving rise to an INP and a GMC (Park *et al.*, 2003; Datta, 1995; Caldwell and Datta, 1998; Boone and Doe, 2008; Bayraktar *et al.*, 2010).

During embryogenesis, the NBs delaminate from the ventral neuroectoderm and, subsequently, form a NB layer between the ectoderm and the mesoderm. In the ventral nerve cord, they are organized within two identical segmental sets, called neuromeres. Each neuromere contains 25 NBs per embryo side. The brain cortex is formed by specific anterior-dorsal NBs of neuroectoderm (procephalic neuroectoderm), while the ventral nerve cord (VNC) is formed by ventral neuroectodermal NBs (Urbach *et al.*, 2003; Younossi-Hartenstein *et al.*, 1996).

During the asymmetric NB's division, the spindle orientation is directed perpendicularly to the plane of the NB layer. Subsequently, the NB progeny (GMCs, immature neurons) forms a distinct stack dorsally of the NB that it originated from. Following a tight series of asymmetric divisions, each NB lineage remains spatially adjacent to the NB progenitor. In this context, brain is formed by NB lineages that are situated externally on its surface, adjacent to the last born (youngest) neurons. Early born neurons and glial cells are the most remote from the NB, bordering the nascent neuropile. CNS histological analysis via stage-specific and cell-specific fluorescent markers addresses the NB proliferation and neuronal differentiation (Brody and Odenwald, 2002).

During embryonic stages 14-15, the primary NBs undergo one last division "pulse", after which only the GMCs divide (time window of 2-3 hours). NBs undergo either apoptosis or mitotic arrest. Only five NBs per brain hemisphere escape the mitotic arrest and proliferate (the four mushroom body NBs, the basal anterior NB). During early larval stages, the surviving NBs undergo a transition from quiescence to activation. Finally, most of the NBs are proliferating during the L3 stage (Ito and Hotta, 1992).

The re-entrance from quiescence (G_0) to the S phase of cell cycle, the number of the upcoming mitotic divisions, and the NBs' life-span are all regulated by certain transcription factors (positive and negative regulators) (Maurange and Gould, 2005;

Bilder, 2001; Doe, 2001). For instance, Hox acts as negative regulator of the NB proliferation inducing the NB apoptosis (proliferative restriction). On the other hand, Trol factor (*Drosophila* homologue of mammalian Perlecan) initiates the NB division and mediates signals through FGF and Hedgehog pathways (Park *et al.*, 2003). In addition, nutrition-derived signal acts via glia-secreted insulin intermediate to control the NB transition from the quiescent to the proliferative state (Sousa-Nunes *et al.*, 2011; Chell and Brand, 2010). Cell-to-cell adhesion molecules also contribute to the NB proliferation. *Drosophila E-cadherin* (*DEcad*) is expressed in NB, secondary neuron and glial cell context with dominant negative *DE-cadherin* leading to reduced NB proliferation and, subsequently, to the absence of neurons and axon tracts (Dumstrei *et al.*, 2003a; Dumstrei *et al.*, 2003b). Grainyhead (Grh) is a transcription factor expressed in all post-embryonic NBs outside the optic lobe that increases *DEcad* expression in proliferating NBs (Almeida and Bray, 2003). Finally, APC1 and APC2 cytoplasmic proteins bind to the cadherin-catenin complex, interfere with Wg/Wnt signaling and as such contribute to the NB proliferation (Akong, 2002). Once neurons of the abdominal neuromeres reach the proper number, *AbdA* expression initiates apoptotic cascades terminating the NB divisions.

1.3. Asymmetric cell division and tumor biology.

The mechanism of asymmetric distribution of the NB components has been extensively studied (Neumüller and Knoblich, 2009; Knoblich, 2008; Wu *et al.*, 2008; Doe, 2008): during late prometaphase, three proteins; Numb (endocytic inhibitor of Notch signaling), Brat (translation inhibitor) and Prospero transcription factor get asymmetrically localized, throughout the basal plasma membrane of each dividing NB (Sonoda and Wharton, 2001; Lee *et al.*, 2006; Bello *et al.*, 2006; Betschinger *et al.*, 2006). Adaptor proteins Miranda and Partner of Numb share common kinetics and localization with BRAT and Numb respectively and, upon binding, they induce their basal accumulation. Miranda binds to BRAT, Partner of Numb binds to Numb and they altogether form a basal crescent. (Lee *et al.*, 2006; Betschinger *et al.*, 2006; Lu *et al.*, 1998; Wang *et al.*, 2007). In type I NBs, Miranda also mediates the transport of the Prospero transcription factor into the GMC (Knoblich *et al.*, 1999; Spana and Doe, 1995). Shortly after the formation of the basal crescent, the mitotic spindle aligns parallel to the apico-basal axis ensuring their inheritance to one of the two daughter cells (the basal GMC). The asymmetric accumulation of basal determinants is

mediated by the proper apical localization of the Par3, Par6 and Bazooka (PDZ domain-containing proteins), aPKC (protein kinase atypical PKC) (Wodarz *et al.*, 1999; Schober *et al.*, 1999) and adaptor protein Inscuteable (Kraut and Campos-Ortega, 1996). In this context, the activated Par6 phosphorylates Lethal giant larvae (Lgl), a cytoskeletal protein that inhibits the aPKC kinase activity during NB interphase. Upon phosphorylation, the Lgl gets substituted by Bazooka in the aPKC complex altering the substrate specificity. As a result, Numb gets phosphorylated and basally accumulated. Furthermore, Inscuetable binds the PAR3–PAR6–aPKC complex to a $G\alpha_i$ Partner of Inscuteable (PINS) complex which acts via Mud and Dlg to anchor the mitotic spindle and align it with the apico-basal axis (Schaefer *et al.*, 2000).

Pathologies that derive from disruption of the aforementioned mechanism have been characterized. Defects in specific genes that regulate asymmetric cell division lead to hyperplasia phenotype; with NBs failing to generate differentiated progeny (GMCs, neurons and glia). Over-proliferated NB-like undifferentiated cells appear in abundance throughout the CNS at the expense of differentiated cells. For instance, loss of function of any of the *l(2)gl*, *dlg*, and *brat* genes produces hyperplasia. The genetic defects that contribute to such tumorigenesis have been first characterized in *Drosophila* before their mammalian homologues were implicated in cancer, highlighting the paramount importance of *Drosophila* model system in cancer studies (Schimanski et al., 2005).

1.4. Notch signaling pathway.

Notch phenotype was first identified in the fruit fly wing near a century ago (Dexter, 1914) and, ever since, Notch signaling pathway has been extensively studied and implicated in wide variety of biological features (e.g. developmental processes, cell-fate determination, tissue homeostasis and certain pathologies). Tightly regulated variable rounds of signaling cascades initiated by a ligand-receptor binding result in transcriptional activation of Notch's target genes repertoire (see section 1.4.1).

Canonical Notch ligands of *D. melanogaster* (Delta, Serrate) form a group of structurally similar transmembrane proteins. Their extracellular domain consists mostly of multiple EGF repeats. The Serrate (and its Jagged orthologues) also contains a cysteine-rich domain. On the other hand, Notch receptor is formed as transmembrane heterodimer with heterodimeric fragments (HDN and HDC) interacting via the cysteine-rich Lin12/ Notch repeats (LNRs) which is called the

negative regulatory region. While inactive, this region holds certain conformation that surrounds the receptor's cleavage recognition site, making it inaccessible to ADAM proteases (Gordon *et al.*, 2007). Upon receptor-ligand binding, the extracellular N-terminal Delta–Serrate–LAG2 (DSL) domains of the ligand contacts the extracellular EGF 11–12 fragment of the receptor, the cleavage site gets exposed to the proteases (mostly ADAM10), and subsequently cleaved (Luca *et al.*, 2015; Cordle *et al.*, 2008; van Tetering *et al.*, 2009). The ADAM-mediated cleavage makes accessible the transmembrane-intracellular fragment of Notch to the γ-secretase complex and enables its intramembrane proteolysis that releases the Notch intracellular domain (NICD) in the cytosol. NICD consists of one single RAM (RBP-jκ Associated Module) domain, seven ankyrin repeats (ANK), a transactivation domain (TAD), and a PEST (proline (P)/glutamic acid (E)/serine (S)/ threonine (T)-rich motif) sequence at the carboxy-terminus. (Kopan and Ilagan, 2009; Kovall and Blacklow, 2010; Nam *et al.*, 2006; Wilson and Kovall, 2006). NICD also carries multiple nuclear localization sequences (NLSs) (Kopan *et al.*, 1994) as well as target sites for multiple post-translational modifications such as phosphorylation (Ramain *et al.*, 2001) and ubiquitination (Fryer *et al.*, 2004).

Notch transduces its signal to the nucleus via the transcription factor CBF1/RBp-Jκ or Su(H) or Lag1 (collectively called CSL). In case of NICD module absence in the nucleus, CSL binds to DNA and recruits transcriptional repressors such as Hairless, CtBP (C-terminal Binding Protein), Groucho, Spen, or others. This provokes a positive feedback loop for histone deacetylase (HDACs) recruitment and, altogether, this contributes to the transcriptional repression of the Notch target genes (Furriols and Bray, 2001; Morel *et al.*, 2001; Kao *et al.*, 1998). On the other hand, when signaling cascade gets activated, NICD translocates into the nucleus. Through its RAM and ANK domains, it interacts with the CSL (Su(H) in *Drosophila*) forming an interface to which the amino-terminus of Mastermind (Mam) binds and the transcriptional repression complex gets disassembled (Morel and Schweisguth, 2000; Barolo *et al.*, 2002; Kopan *et al.*, 1994).. This cascade of events locks the complex into its active conformation and transcription gets initiated (Nam *et al.*, 2006; Wilson and Kovall, 2006). The target genes recruit an activation complex which includes histone acetyltransferases (HATs) and chromatin remodeling complexes (Kurooka and Honjo, 2000; Wallberg *et al.*, 2002; Fryer *et al.*, 2002).

However, this is a dynamic process since, when in need, Notch signaling may "switch off". NICD can be inactivated via cyclin-dependent kinase-8 (CDK8) phosphorylation, leading to E3-ubiquitin-ligase-dependent poly-ubiquitination and subsequently proteasome-mediated degradation (Fryer *et al.*, 2004; Hubbard *et al.*, 1997).

1.4.1. Notch target genes.

Although the Notch signaling target genes are expressed in a cell-type specific context, there are several common target genes (Bjornson *et al.*, 2012; Mourikis *et al.*, 2012; Vasyutina *et al.*, 2007). The most well-examined examples are the *Drosophila* proteins Enhancer of split (E(spl)), homologues to human HES (Jarriault *et al.*, 1998). HES share the following features: (i) a basic helix-loop-helix (b-HLH) domain, (ii) a WRPW motif, and (iii) an "orange domain". b-HLH domain acts as direct repressor of transcription due to its DNA-binding capacity.

Furthermore, many other target genes have been identified, including cyclin D1 (Ronchini *et al.*, 2001), NRARP (Lamar *et al.*, 2001), NF-κB (Vilimas *et al.*, 2007), p21 (Rangarajan *et al.*, 2001) and pre-Tα (Reizis *et al.*, 2002) in different contexts. Interestingly, Certain target genes have distinct role in tumor formation such as MYC (Weng *et al.*, 2006; Klinakis *et al.*, 2006; Palomero *et al.*, 2006), IGF1-R (Eliasz *et al.*, 2010), survivin (Chen *et al.*, 2011) and Snail homolog 2, commonly known as SLUG (Niessen *et al.*, 2008).

1.4.2. Notch Signaling contribution to NB lineage cell-fate determination.

Notch signaling pathway is implicated in just about any cell-fate determination event in metazoan development, "safe-guarding" both lineage-specific differentiation and stem cell self-renewal in many tissues, including the CNS (Artavanis-Tsakonas *et al.*, 1995; Kopan and Ilagan, 2009). In particular, during CNS development, more cells than necessary share equal potential of obtaining a terminally differentiated cell fate. Notch signaling balances this tendency by dictating the neural-epidermal fate determination. Proneural cell clusters share neural-committing potential thanks to the expression of b-HLH transcriptional activators (proneural proteins). However, Notch signaling represses the expression (activity) of proneural genes in favor of preventing equipotent proneural cells from all acquiring the same fate, ('inhibitory Notch signaling') (Parks et al., 1997). On the other hand, cells that escape from Notch

signaling boost the expression of proneural proteins and, thus, they acquire a differentiated identity (neuroectodermal to NB fate). In fact, forced expression of E(spl) b-HLH repressors is sufficient to inhibit neural development (Nakao and Campos-Ortega, 1996). In *Drosophila*, neural repression mediators are encoded by the *Enhancer of split* complex (*E(spl)*). Notch signaling in vertebrates also represses neurogenesis and myogenesis via HES repressors (mammal), also known as HER (fish) or ESR (frog) (Chitnis et al., 1995).

1.4.3. Notch signaling and tumorigenesis.

The kinetics of the NICD module get positively and negatively regulated by more than one "checkpoints"; e.g. proteolysis, glycosylation, ubiquitylation and/ or phosphorylation of itself or interacting proteins mediating its function. However, in case of the NICD's aberrant activation or repression, cancerous phenotypes may arise in a variety of tissues due to (i) overexpression of either ligands or factors that activate the Notch receptor(s), (ii) loss of its negative regulators, and (iii) post-translational modifications (e.g. O-fucosylation, ubiquitination) of either receptor or ligand (Haines and Irvine, 2003; Lei *et al.*, 2003; Okajima and Irvine, 2003 Fryer *et al.*, 2004). Tumorigenesis due to deregulation of Notch has been mostly studied in mammalian tumor formation (hematopoietic tumors, solid tumors etc.). For instance, a large percentage of T cell acute lymphoblastic leukaemia (T-ALL) patients bear Notch mutations that trigger a constitutively active Notch pathway. Interestingly though, depending on the cellular context, impaired Notch pathway contributes either to oncogenesis or tumor suppressing (Ntziachristos *et al.*, 2014).

1.5. Notch signaling implication in the *D. melanogaster* developed cancer model.

Recent work addresses the contribution of Notch signaling during *Drosophila* larval neurogenesis as a valuable system for elucidating the balance between NB self-renewal and differentiation (Zacharioudaki *et al.*, 2012; Zacharioudaki *et al.*, 2016; Magadi *et al.*, in preparation). In the CNS context, ectopically overactivated Notch's target genes have been implicated in hyperplasia generation (NB-lineage-specific expression of *E(spl)mγ*, *E(spl)mβ*, *E(spl)m8* and *deadpan* (*dpn*)). Dpn b-HLH-O protein contributes to repressing the differentiation status of the CNS. The overexpression of *E(spl)mγ*, *dpn* or *klu* is sufficient to cause NB hyperplasia (Berger *et al.*, 2012; San-Juán

and Baonza, 2011; Xiao *et al.*, 2012; Zacharioudaki *et al.*, 2012; Magadi *et al.*, in preparation).

Aberrant expression of Notch target genes through CNS generates a phenotype that tilts the scales in favor of the undifferentiated cell-state and compromises the organism survival towards adulthood. Transcriptomic analysis of the hyperplastic CNSs has revealed a network of transcription factors that, in case of aberrant Notch activity, contributes to the promotion/ maintenance of the hyperplastic state: (i) NB stemness regulators: *grh*, *E(spl)mγ*, *dpn*, *klu*, and (ii) NB temporal temporal regulators: *svp*, *cas*, *hth* (Zacharioudaki *et al.*, 2016). The Notch hyperactivation in the NB lineage not only compromises the cell-fate commitment towards the GMCs and neurons/ glial cells, but also causes the dedifferentiation of the already differentiating GMCs and INPs towards the NB state.

In comparison to the *E(spl)mγ*, *dpn*-derived hyperplastic CNSs, Notch's constitutive activity leads to hyperplastic CNS of distinct transcriptomic content (Magadi *et al.*, in preparation). This could be due to abnormal overexpression of the whole *E(spl)* target genes repertoire as well as all other hyperplasia promoting transcription factors (e.g. Dpn, Klu, Grh, Svp) (Zacharioudaki *et al.*, 2016).

Interestingly, a major novel finding of our research suggests that Notch-hyperactivation in NB progeny leads to CNS hyperplastic tissue that is also capable of neoplastic transition (Magadi *et al.*, in preparation). The latter, not only emphasizes the *Drosophila*'s role in malignancy studies, but also introduces a whole new perspective in Notch's implication in carcinogenesis. In summary, the hyperplastic CNSs, once allografted in a wild-type host ("allograft assay", see below), lead to tumor outgrowth *in vivo*. However, the transcriptome "signature" of the tumor allografts has yet to be addressed.

2. Materials and methods.

2.1. *Drosophila melanogaster* stocks.

	Genotype	Reference
1	*y*; *UAS-Notch$^{\Delta E}$/ UAS-Notch$^{\Delta E}$*; +/ +	Fuerstenberg and Giniger, 1998
2	*yw*; *UAS-E(spl)mγ UAS-Dpn/ CyO Tb* ; +/ +	Magadi *et al.*, in preparation
3	*hsFLP*; +/ +; *act5C-FRT-stop-FRT-Gal4 UAS-nlsEGFP/ TM6B*	Magadi *et al.*, in preparation
4	*yw*; *UAS-EGFP-6xmycNLS^{GO6}/ CyO*; +/ +	Wang and Struhl, 2005
5	*w^{1118}*; +/ +; +/ +	Ambegaokar and Jackson, 2010
6	*yw nanos>integrase*; *y^{+}{attP40}/ y^{+}{attP40}*; +/ +	Groth *et al.*, 2004 Markenstein *et al.*, 2008
7	*yw*; *Cyo/ sna^{Sco}*; +/ +	Kenneth Tartof, Fox Chase Cancer Center
8	*w^{1118}*; *w^{+} lov91Y-Gal4/ w^{+} lov91Y-Gal4*; +/ +	Manseau *et al.*, 1997
9	*yw*; *y^{+}{U-NPDG w^{+}}/ y^{+}{ U-NPDG w^{+}}*; +/ +	This study
10	*tub-Gal80^{ts}/ y FM7 act5C-GFP*; +/ +; *grh-Gal4/ TM6B*	Zacharioudaki *et al.*, 2016

2.2. *Drosophila melanogaster* genetics.

2.2.1. Hyperplastic central nervous system generation.

Hyperplastic late L3 CNSs were generated according to the following established genetic scheme (Magadi *et al.*, in preparation): *y; UAS-Notch$^{\Delta E}$/ UAS-Notch$^{\Delta E}$; +/ +* and *yw; UAS-E(spl)mγ UAS-Dpn/ CyO Tb ; +/ +* females were crossed to *hsFLP*; +/ +; *act5C-FRT-stop-FRT-Gal4 UAS-nlsEGFP/ TM6B* male individuals. In this context, *actin5C* promoter was activated in random neuroblast clones, upon heatshock-induced FLP recombination ("FLP-out" approach of an *act5C-FRT-stop-FRT-Gal4* transgene, where "*FRT*" is the FLP Recombination Target and "*stop*" signifies a polyadenylation site). As such, randomly FLP-ed-out *Notch$^{\Delta E}$*- double *HES*-overexpressing *E(spl)mγ Dpn*-overexpressing cells were made to co-express a fluorescent marker (*UAS-nlsEGFP*) in order to be distinguishable from surrounding wild-type tissue. Crosses were kept at 25^{o}C for 5 days, and the progeny was heat shocked (37^{o}C, 1 hour) 3 days prior to dissection.

2.3. Tissue allograft method.

Hyperplastic late L3 CNSs were generated as previously described (see section 2.2.1).

On the other hand, outgrowing tumors were generated within healthy hosts utilizing tissue the "tissue allograft method", obtained by E. Gateff (Gateff, 1994) and recently revived by the C. Gonzalez laboratory (Rossi and Gonzalez, 2015). In detail, hyperplastic brain lobes of the late L3, female, non-*Tb* progeny of the aforementioned crosses (see section 2.2.1) were isolated (in filter sterilized 1xPBS) and individually injected in the abdomen of recently eclosed, nutritionally supplemented female individuals (w^{1118}/ w^{1118}; +/ +; +/ +) (as described in Rossi and Gonzalez, 2015). As such, we generated the first allograft passage individuals (T_0) and after 10-12 days screened for tumor outgrowth *in vivo* thanks to *nlsEGFP* expression (Figure 6). Out of the *nlsEGFP* positive individuals, the tumor tissue was isolated (in filter sterilized 1xPBS), the total RNA was extracted (TRIzol reagent, Thermo Fisher Scientific™ according to manufacturer's instructions) and a part of tumor specimens was re-allografted into new w^{1118} individuals generating the next allograft passage (T_1). Note that each allograft passage individual apart from the T_0 (T_1, T_2, T_3 and so on) was generated out of allografted tumor specimens as injection material, as opposed to T_0 individuals that were allografted with hyperplastic primary brain lobes instead.

2.4. DNA oligos list.

	Oligo name:	Sequence (5'→ 3'):
1	*UAS_EcoRI_F*	CGTACGAATTCGCTTCTGCATGAGCTCGGATC
2	*UAS_EcoRI_R2*	TTTTTGAATTCCTAGACAGGCCTCGATAATTCCCA
3	*NICD_XbaI_F*	CCTCTAGAATGCAATCGCAGCGCAGCCG
4	*NICD_BglII_R*	CAAGATCTGTAGATGGCCTCGGAACCCTTGTTAGCC
5	*pMT_ΔECN_1*	CCACCTGCTTGTTGAGATTCCG
6	*pMT_ΔECN_2*	CGGTGGCCATCAGGCTAACAAG

2.5. Plasmid vector list.

	Plasmid	Reference
1	*pMT_NDecd*	Eastman *et al.*, 1997
2	*pTMW*	Murphy, unpublished data
3	*HSB_dGS*	Piwko, unpublished data
4	*78SB*	Piwko, unpublished data

5	*tdTom FRT*	Tzumin Lee laboratory
6	*P2A_pBMEFRT-p2A-DsRed*	Alwes *et al.*, 2016
7	*NDecd_p2A (N2A)*	This study
8	*HSB_Ger1*	This study
9	*HSB_Ger3*	This study
10	*HSB_Ger4*	This study
11	*HSB_UNPDG*	This study

2.6. DNA Manipulations.

2.6.1. *Drosophila melanogaster* genomic DNA extraction.

For each genomic DNA sample, 30 female adult flies were collected into a 1.5mL microcentrifuge tube and stored at -80^{o}C overnight. 250uL of [Tris HCl 0.1M (pH 9.0) EDTA 0.1M SDS 1%] solution were added and flies were homogenized, at 4^{o}C. Homogenized sample was heatshocked at 70^{o}C for 30 minutes. 56uL KAc 5M were added, the sample got shaked, put on ice for 30 minutes and, then, centrifuged at 13.000rpm for 15 minutes (4^{o}C). Supernatant was transferred into a new 1.5mL microcentrifuge tube and resuspended in 1 volume of Phenol : Chloroform mix (1:1). Resuspension was centrifuged at 13.000rpm for 5 minutes (4^{o}C), supernatant was, once again, resuspended in 1/10 volume isopropanol and centrifuged at 10.000rpm for 5 minutes (4^{o}C). Supernatant was discarded and pellet was washed in 1mL EtOH 70%. Sample was centrifuged at 13.000rpm for 5 minutes (4^{o}C), pellet got air-dried and, finally, resuspended in 100uL distilled water. Concentration of extracted genomic DNA was estimated after 12-16 hours storing at 4^{o}C (Nanodrop).

2.6.2. DNA electrophoresis on an agarose gel.

Agarose gel electrophoresis was performed for the analysis of the size and conformation of DNA in a sample, quantification of DNA according to λ DNA/StyI ladder, and finally the separation and extraction of DNA fragments. 0.8-1.2% agarose was dissolved in 0.5x TAE, which contained ethidium bromide (EtBr). In order to determine both the size and concentration of each DNA sample, λ DNA/StyI ladder of known concentration was loaded along with the samples. Gels were run at 80-110mV, depending on the molecular weight of loaded samples and downstream applications. When adequate migration had occurred, the gel was exposed to UV light with a UV

transilluminator. Thus, the DNA bands were visualized and photographed due to the intercalating fluorescent dye (Ethidium Bromide).

2.6.3. Restriction Endonuclease digestion.

Restriction endonucleases bind and cleave DNA at specific target sequences. DNA was digested by restriction endonucleases to yield DNA fragments of convenient sizes for specific downstream manipulations. In particular, the appropriate amount of DNA was incubated with 1u restriction enzyme, 1x restriction enzyme buffer and distilled water to a final volume of 15-20ul. The incubation temperature and time period were specified by the manufacturer (New England Biolabs, Minotech). Digested DNA was finally analyzed by agarose gel electrophoresis.

2.6.4. Polymerase Chain Reaction (PCR).

Since *Notch*$^{\Delta E}$ and *UAS* PCR amplified fragments were to be cloned, high fidelity proofreading Kapa HiFi DNA polymerase (Kapa Biosystems) was used in order to reduce the error frequency. *pMT_NDecd* and *pTMW* plasmid DNA were used as templates (total amount 0.25ng) for *Notch*$^{\Delta E}$ and *UAS* fragments respectively. Note that the following formula was used for estimating the T_m of the primers (on each PCR reaction):

$$\mathrm{Tm} = 69.3 + 0.41(\mathrm{GC\%}) - 650/\mathrm{L}$$

XbaI and *BglII* restriction sites have been introduced upstream and downstream of *Notch*$^{\Delta E}$ amplified fragment respectively (oligos 3, 4, see section 2.4). The following PCR cycle program has been used:

***Notch*$^{\Delta E}$** (3.2kb)

Initial Denaturation	95°C		3 minutes
Denaturation	98°C		20 seconds
Annealing	65°C		15 seconds
Extension	72°C		3 minutes 12 seconds
Cycles Number		20	
Final Extension	72°C		3 minutes 30 seconds

EcoRI restriction sites have been introduced upstream and downstream of *UAS* amplified fragment (oligos 1, 2, see section 2.4). The following PCR cycle program has been used:

UAS (428bp)			
Initial Denaturation	95^{o}C		3 minutes
Denaturation	98^{o}C		20 seconds
Annealing	60^{o}C		15 seconds
Extension	72^{o}C		15 seconds
Cycles Number		30	
Final Extension	72^{o}C		1 minute

2.6.5. DNA Ligation.

Ligation reactions were based on T4 DNA Ligase^{TM} (New England Biolabs, Minotech) activity and were performed for sticky-end cloning manipulations. Each reaction (the reagents of which were calculated on enzyme manufacturer's instructions or on "NEB^{TM} calculator") was gently mixed and incubated at 18^{o}C overnight. Part of the ligation product (50-100ng) was then transformed in *E. coli* DH5α chemically-induced competent cells.

2.7. *Escherichia coli* manipulations.

2.7.1. *Escherichia coli* transformation.

Competent DH5a *E.coli* cells were taken out of -80^{o}C freezer and thrawn on ice for 5 minutes. The DNA to be transformed was mixed in 100uL of competent cells aliquot in 1.5mL tube and then placed on ice for 20 minutes. Each transformation tube was heat-shocked at 42°C for 90 seconds. 0.6mL LB was then added in each tube and tubes were incubated at 37^{o}C for 45 minutes (outgrowth period). Each transformation tube was centrifuged at 13.000rpm for 18 seconds, RT and cell pellet was resuspended at LB remains. Resuspended pellet was finally plated on LB agar plate (containing the appropriate antibiotic, in our case ampicillin, *100ug/mL*) which was incubated at 37^{o}C, overnight. After, 12-16 hours transformants were counted and isolated for specific downstream manipulations (e.g. Plasmid extraction).

2.7.2. Plasmid purification (small scale).

One single amp^{R} *E.coli* colony, was inoculated to 2mL LB ampicillin-containing (100ug/mL) liquid medium and incubated overnight on a rotary shaker at 165rpm, 37^{o}C. After 12-16 hours, cell culture was transferred to a 1.5mL microcentrifuge tube, under sterile conditions. Plasmid extraction was performed via "NucleoBond® Xtra Midi / Maxi" Macharey Nagel™ reagents according to manufacturer's instructions (with final yield 200-600ng/uL). Plasmid DNA was analyzed by agarose gel electrophoresis. Note that the above mentioned protocol is appropriate for diagnostic purposes (e.g. restriction endonuclease digestion) but no further purposes (e.g. cloning), lacking several purification steps (e.g. column purification).

2.7.3. Plasmid purification (large scale).

One single amp^{R} E.coli colony, was inoculated to 200mL LB ampicillin-containing (100ug/mL) liquid medium and incubated overnight on a rotary shaker at 165rpm, 37^{o}C. After 12-16h, bacterial culture was transferred to 50mL falcons, under sterile conditions and cells were harvested after centrifugation (3000rpm, 4^{o}C). Plasmid extraction was performed via "NucleoBond® Xtra Midi / Maxi" Macharey Nagel™ protocol according to manufacturer's instructions (with final yield 1,500-2,500ng/uL). Plasmid DNA was analyzed by agarose gel electrophoresis.

2.8. *Drosophila melanogaste*r manipulations.

2.8.1. Immunohistochemistry: 3rd instar larval tissues and adult tissues.

Fixation and immunochemistry of both 3rd instar larval and adult tissues was performed according to standard protocols. Primary antibodies were rat-a-Elav, mouse-a-Repo, rabbit a-GFP, mouse a-Prospero (1:50), guinea pig a-Deadpan (1:3.000) and rabbit a-Asense (1:1000) diluted in PBT (PBS, BSA, Triton-X solution). Secondary antibodies were conjugated to Alexa488, 555, 647, Cy3 Fab 555 (Molecular Probes). Brain fixed samples were imaged on Leica SP8 confocal microscope (IMBB, FORTH).

2.9. *UAS-FRT-Notch$^{\Delta E}$-2A-DsRed-FRT-nlsEGFP* construct molecular cloning.

The transgene of interest was cloned in an *attB*-containing *D. melanogaster* transformation vector in five steps. *HSB_Ger1*, *HSB_Ger3*, *HSB_Ger4*, *NDecd_p2A (N2A)*, and *HSB_UNPDG* plasmid vectors were constructed (see section 2.5) and finally *HSB_UNPDG* plasmid vector (carrying the transgene of interest) was utilized for downstream manipulations (see section 3.2). In detail, *HSB_UNPDG* plasmid vector of 14.640bp total size contained (i) the *UAS-FRT-Notch$^{\Delta E}$-2A-DsRed-FRT-nlsEGFP* transgene (plasmid coordinates: 1.573-4.770), (ii) a *mini-white^{+}* dominant gene for transgenic selection (plasmid coordinates: 8.153-11.038), and (iii) the *attB* locus (plasmid coordinates: 1-279) for integration within the *attP40* genomic locus of the recipient injected line (Fish *et al.*, 2007). *UAS-FRT-Notch$^{\Delta E}$-2A-DsRed-FRT-nlsEGFP* transgene features shared the following plasmid coordinates:

***U-NPDG* transgene feature:**	**Plasmid coordinates: (bp)**
UAS	1.103-1.467
FRT	1.525-1.558
Notch$^{\Delta E}$	1.573-4.770
P2A	4.771-4.836
DsRed	4.852-5.532
SV40 termination signal	5.533-5.761
FRT	6.486-6.519
nls-EGFP	6.561-7.394
SV40 termination signal	7.424-7.610

All the developed plasmids in this study (see section 2.5) were generated according to molecular cloning standard protocols. *HSB_dGS* plasmid of 9.339bp total length (BamHI: 1.048 site, AgeI: 1.248 site) was BamHI/ AgeI digested and a linearized vector of 9.139bp total length was isolated. *78SB* plasmid of 12.599bp total length (BglII: 1.845 site, AgeI: 4.134 site) was BglII/ AgeI digested and an insert fragment of 2.289bp total length was isolated. BglII/ AgeI *78SB* insert fragment was cloned into BamHI/ AgeI digested *HSB_dGS* linearized vector in order to develop *HSB_Ger1* plasmid (11.428bp total length). Note that BglII digested products share compatible sticky ends to BamHI sticky ends that result in a successful ligation.

HSB_Ger1 plasmid of 11.428bp total length (Acc65I: 94, 2.128, 9.206 sites) was Acc65I digested and a linearized vector of 9.206bp total length was

dephosphorylated and isolated according to standard protocols. *tdTom FRT* plasmid of 5.471bp total length (Acc65I: 201, 2.720 sites) was Acc65I digested and an insert fragment of 2.519bp total length was isolated. Acc65I digested *tdTom FRT* insert fragment was cloned into Acc65I digested *HSB_Ger1* linearized vector in order to develop *HSB_Ger3* plasmid (11.725bp total length).

HSB_Ger3 plasmid of 11.725bp total length (EcoRI: 1.070 site) was EcoRI digested and a linearized vector of 11.725bp total length was isolated and dephosphorylated according to standard protocols. *pTMW* plasmid of 11.021bp total length was used as template to amplify via PCR a UAS-containing fragment flanked by EcoRI restriction sites (*pTMW* plasmid coordinates of PCR product: 2.996-3.423). Note that the *UAS per se* was a 365bp fragment within the PCR product itself (*pTMW* plasmid coordinates of UAS: 3.024-3.388). EcoRI digested *UAS*-containing PCR product was used as an insert and cloned into EcoRI digested *HSB_Ger3* linearized vector in order to develop *HSB_Ger4* plasmid of 12.158bp total length.

A truncated derivative of the *D. melanogaster* Notch receptor, constitutively susceptible to the γ-secretase-mediated S3 cleavage ($Notch^{\Delta E}$) was amplified via PCR using *pMT_NDecd* plasmid as template and used as insert. $Notch^{\Delta E}$ derivative (3.182bp length) encoded for the translation start site, the exons 1 and 2 (containing signal peptide for membrane translocation), the exon 6 (containing transmembrane domain, RAM domain, ankyrin repeats, the *Su(H)* binding site), and finally exons 7, 8, 9 (containing TAD and PEST domains). However, it lacked the exons 3, 4, 5 (containing the EGF-like repeats 11 and 12 signal cleavage site). It also lacked the final two codons (isoleucine-encoding and TGA stop codon) in order to be cloned in frame with *p2A* and *DsRed* coding sequence. *P2A_pBMEFRT-p2A-DsRed* plasmid of 4.061bp total length (XbaI: 139, 212 sites, BamHI: 253 site) was XbaI/ BamHI digested and a linearized vector of 3.947bp total length was dephosphorylated and isolated according to standard protocols. XbaI and BglII-flanked (at 5' and 3' respectively) $Notch^{\Delta E}$ PCR-amplified fragment that used as insert was cloned in the XbaI/ BamHI digested *P2A_pBMEFRT-p2A-DsRed* vector in order to develop *NDecd_p2A (N2A)* plasmid of 7.157bp total length.

HSB_Ger4 plasmid of 12.158bp total length (NheI: 1.568 site, MluI: 3.282 site) was NheI/ MluI digested and a linearized vector of 10.444bp total length was dephosphorylated and isolated according to standard protocols. *NDecd_p2A (N2A)* plasmid of 7.157bp total length (XbaI: 140 site, BssHII: 31, 4.336, 4.394 sites) was

XbaI/ BssHII digested and an insert of 4.196bp total length was isolated. XbaI/ BssHII *NDecd_p2A (N2A)* insert fragment was cloned in NheI/ MluI digested *HSB_Ger4* linearized vector in order to develop *HSB_UNPDG* plasmid of 14.640bp total length. Note that NheI digested products share compatible sticky ends to XbaI sticky ends that result in a successful ligation. Likewise, MluI digested products share compatible sticky ends to BssHII sticky ends that result in a successful ligation.

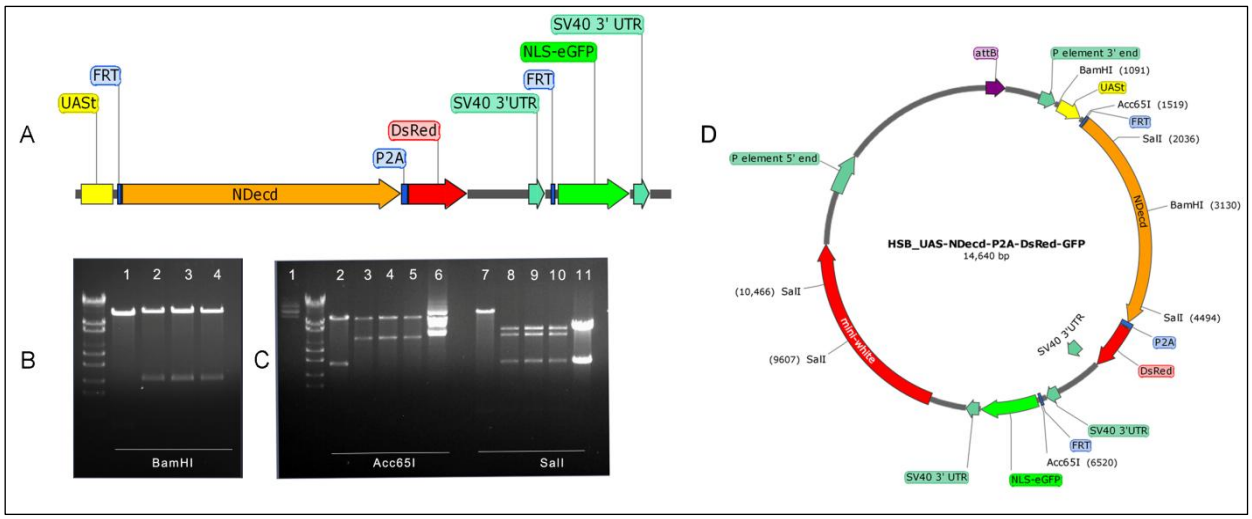

Figure 1. ***UAS-FRT-Notch$^{\Delta E}$-2A-DsRed-FRT-nlsEGFP*** **transgene construction. A.** Transgene *UAS-FRT-Notch$^{\Delta E}$-2A-DsRed-FRT-nlsEGFP* map. **B**, **C.** BamHI, Acc65I, SalI screening for *HSB_UNPDG* plasmid (lanes 2, 3, 4 as opposed to control HSB_Ger4 clone in lane 1). **D.** HSB_UNPDG plasmid map.

3. Results.

3.1. *UAS-FRT-Notch$^{\Delta E}$-2A-DsRed-FRT-nlsEGFP* transgene development.

Both the hyperplastic (Zacharioudaki *et al.*, 2012; Zacharioudaki *et al.*, 2016) and the malignant capacity (Magadi *et al.*, in preparation) of Notch-hyperactive CNSs have been addressed. In our study, we introduced the hypothesis that there may be a *Notch$^{\Delta E}$*-derived tumor progression stage, after which *Notch$^{\Delta E}$* expression is no longer necessary to sustain tumor propagation. In order to study the latter, *UAS-FRT-Notch$^{\Delta E}$-2A-DsRed-FRT-nlsEGFP* transgene was developed (see section 2.9, Figure 1) in order to (i) firstly induce *Notch$^{\Delta E}$*-derived hyperplasia, (ii) monitor such hyperplasia via DsRed fluorescent marker, (iii) take advantage of the *hsFLP – FRT* recombination "at will" to precisely excise the *Notch$^{\Delta E}$* from its genomic locus, and finally (iv) monitor the excision events via nlsEGFP fluorescent marker (Figure 2).

In the first step, we developed *HSB_Ger1* plasmid (for details see section 2.9). *HSB_dGS* plasmid was BamHI/ AgeI double digested to excise out the *hsp70* promoter region (*HSB_dGS* plasmid coordinates: 1.059-1.191) which got replaced by a *CRM1*-containing fragment. The latter was subcloned from the BglII/ AgeI digested *78SB* plasmid.

In the second step, we developed *HSB_Ger3* plasmid (for details see section 2.9). *HSB_Ger1* plasmid was Acc65I digested to excise out the *CRM1*-sub-containing fragments (*HSB_Ger1* plasmid coordinates: 1.087-3.215 and 3.215-3.309) which got replaced by a *FRT-myr-tdTomato*-containing fragment. The latter was subcloned from the Acc65I digested *tdTom FRT* plasmid.

In the third step, we introduced a *UAS*-containing fragment in the *HSB_Ger3* plasmid and developed *HSB_Ger4* plasmid (for details see section 2.9). *HSB_Ger3* plasmid was linearized by EcoRI digestion and *UAS* PCR-amplified fragment flanked by EcoRI sites (both at 5' and 3' ends) was cloned in between according to standard protocols (for PCR amplification protocol see section 2.6.4).

In the fourth step, we introduced a PCR product that contained the *Notch$^{\Delta E}$* truncated form of Notch receptor in the *P2A_pBMEFRT-p2A-DsRed* plasmid and developed *NDecd_p2A (N2A)* plasmid (for details see section 2.9). *P2A_pBMEFRT-p2A-DsRed* plasmid was BamHI/ XbaI digested and the *Notch$^{\Delta E}$* PCR-amplified fragment (flanked by XbaI and BglII at 5' and 3' ends respectively) was cloned in

frame to *p2A-DsRed* CDS according to standard protocols (for PCR amplification protocol see section 2.6.4).

In the final step, we developed the *HSB_UNPDG* plasmid (for details see section 2.9). *HSB_Ger4* plasmid was NheI/ MluI digested to excise out the *myr-tdTomato*-containing fragment (*HSB_Ger4* plasmid coordinates: 1.568-3.282) which got replaced by the *Notch$^{\Delta E}$-p2A-DsRed*-containing fragment. The latter was subcloned from the XbaI/ BssHII digested *NDecd_p2A (N2A)* plasmid.

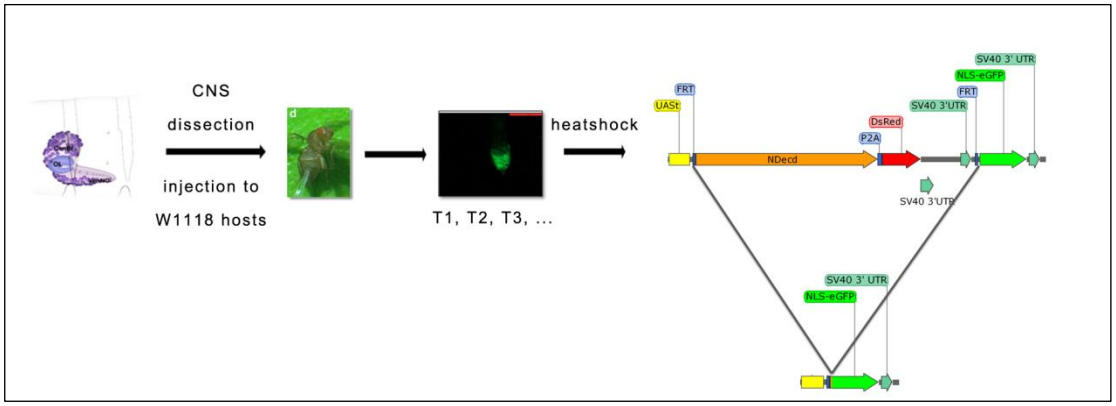

Figure 2. Proposed genetic scheme to address the Notch role in sustaining tumor growth. *UAS-FRT-Notch$^{\Delta E}$-p2A-DsRed-FRT-nlsEGFP* (*U-NPDG*) transgenic line shares the dual capacity of both CNS hyperplasia induction (UAS-Gal4-mediated overexpression) and its genotypic excision *in locus* (*FLP-FRT*-based). Upon removal of Notch hyperactivity, tumor reversion potential and its temporal dynamics are yet to be specified.

3.2. *Drosophila melanogaster UAS-NPDG* transgenic line development.

HSB_UNPDG plasmid DNA was injected (0.4-0.5ug/uL) and transformed in *yw*; *nanos>integrase*; *y^{+}{attP40}*/ *y^{+}{attP40}*; +/ + recipient line embryos (as previously described by Groth *et al.*, 2004; Bischof *et al.*, 2007) and the eclosed G_0 individuals were crossed to the *yw*; *Cyo*/ *sna^{Sco}*; +/ + carrying a balancer for the second chromosome. The two G_1 transgene-carrying adults were individually crossed to the *yw*; *Cyo*/ *sna^{Sco}*; +/ + line and their G_2 progeny were screened for the *mini-white^{+}* dominant phenotype. As a result, the homozygous transgenic line (*yw*; *y^{+}U-NPDG}*/ *y^{+}{U-NPDG};* +/+) was developed via successive counter-selection of balancer-carrying (*CyO*) individuals (Figure 3).

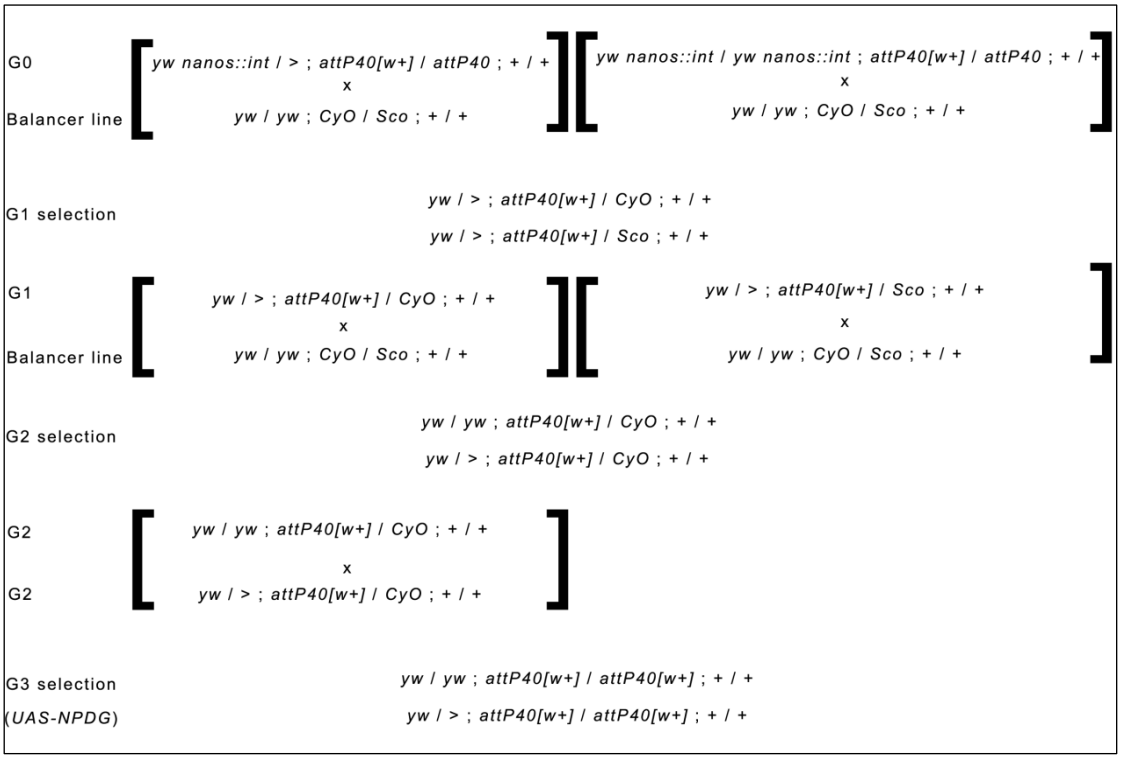

Figure 3. *D. melanogaster* genetic scheme for *yw; y^{+}U-NPDG}/ y^{+}{U-NPDG}; +/+* transgenic line development.

3.3. Aberrant Notch signaling generates CNS hyperplasia in UAS-NPDG transgenic *D. melanogaster* line.

Published results of Zacharioudaki and colleagues documented that hyperplastic CNS generation when a NB-specific Gal4 drives *UAS-Notch$^{\Delta E}$* expression (Zacharioudaki *et al.*, 2012). However, since we developed a different *Notch$^{\Delta E}$* truncated derivative (encoding similar but not identical open reading frame compared to the previously used; described in Fuerstenberg and Giniger, 1998), we aimed to address the extent (if any) that *UAS-NPDG* expression also caused larval hyperplastic CNSs when combined with proper *Gal4*-expressing driver line.

In our study, we postulate that the aberrant Notch signaling in the larval NBs and their immediate GMC progeny (*UAS-NPDG* overexpression) is sufficient to drive NB overproliferation and, subsequently, hyperplasia (Figure 5).

The *Notch$^{\Delta E}$* CDS of *UAS-NPDG* transgene was overexpressed following the *grh-Gal4* spatiotemporal expression pattern. *grainyhead* (*grh*) is expressed in most of the post-embryonic NBs and their immediate GMC progeny outside the optic lobe (Prokop *et al.*, 1998; Zacharioudaki *et al.*, 2012) (Figure 4). However, given the fact

that the aberrant Notch signaling activity in a *grh-Gal4* manner was lethal even before late L2 larval stage, we took advantage of a *Gal80^{ts}*-expressing line (Gal80^{ts}: temperature-sensitive inhibitor of Gal4) in order to develop conditional *UAS*-driven overexpression of *Notch$^{\Delta E}$* in distinct time-points of larval life (Zacharioudaki *et al.*, 2012). We crossed *tub-Gal80^{ts}/ >; +/ +; grh-Gal4/ TM6B* male to *yw/ yw*; *y^{+}{U-NPDG}/ y^{+}{U-NPDG}; +/+* female individuals at 18^{o}C, and performed a temperature shift from 18^{o}C to 30^{o}C ten days later (24 hours prior to dissection) in order to degrade the Gal80^{ts} inhibitor of Gal4. After 24 hours, we performed α-Dpn histological analysis of CNS in the late L3, female, non-*TM6B* progeny according to the standard protocols (see section 2.8.1). We observed a significant overproliferation of both the Type I and Type II neuroblasts (Figure 5). We reasoned that combined with *Gal80^{ts}*, the *grh-Gal4*-expressing line (*tub-Gal80^{ts}/ FM7 act5C-GFP; +/ +; grh-Gal4/ TM6B*) indeed provoked NB hyperplasia through the whole CNS (outside the optic lobe).

However, although *DsRed* CDS was cloned in frame with p2A (Figure 4), we did not observe any *DsRed* endogenous expression in neither of the contexts that we screened. At first, we crossed *UAS-NPDG* line with the *TDC2-Gal4*-expressing line. TDC2 stands for Tyrosine Decarboxylase 2, part of octopamin-producing pathway. TDC2 expression pattern locates in the midline of the larval CNS (data not shown). Furthermore, we crossed *UAS-NPDG* line with *tub-Gal80^{ts}/ FM7 act5C-GFP; +/ +; grh-Gal4/ TM6B* line (18^{o}C/ 25^{o}C without temperature shift, and 18^{o}C to 30^{o}C temperature shift).

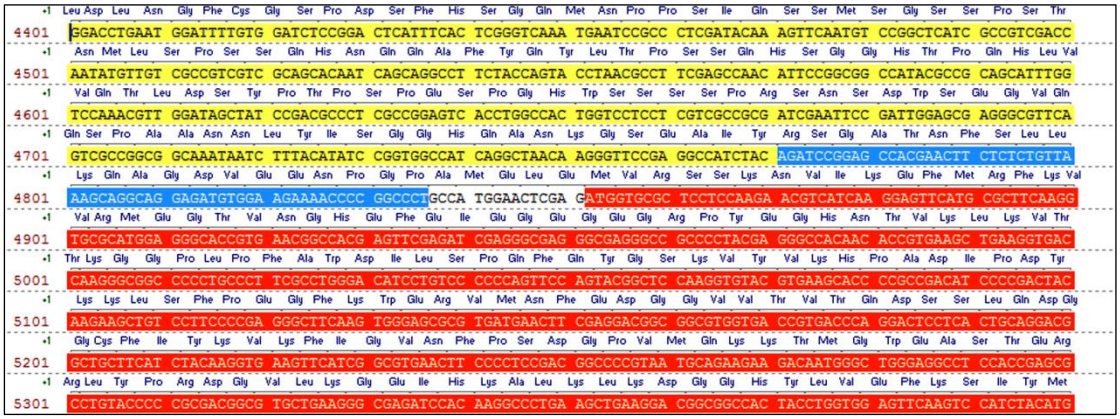

Figure 4. Sequencing results of *Notch$^{\Delta E}$-p2A-DsRed* junction. Part of *Notch$^{\Delta E}$* (3' end) is depicted in yellow color, p2A is depicted in blue, and part of *DsRed* (5' end) is depicted in red color. Note the intactness in the frame.

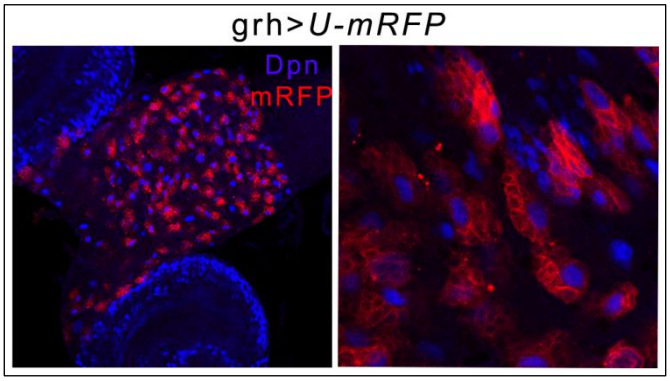

Figure 5. Expression pattern of *grh-Gal4*-expressing driver line. *grh-Gal4* is expressed in the neuroblasts and their immediate progeny (GMCs). Under wild-type conditions, *deadpan* marks the neuroblasts but not in their progeny.

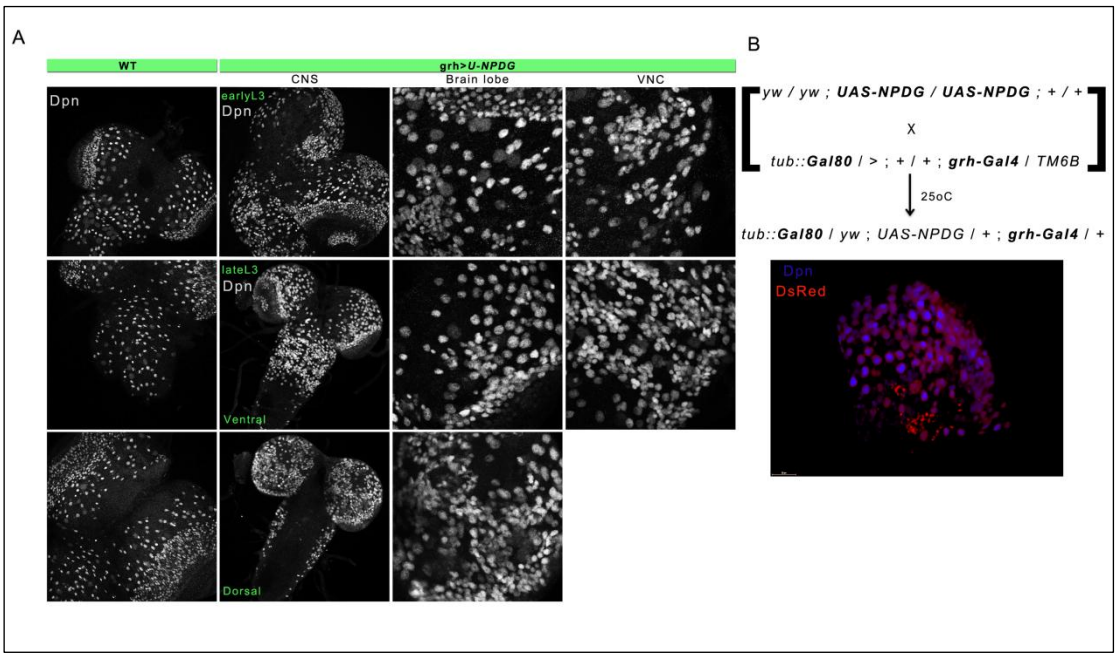

Figure 6. Notch hyperactivation (*U-NPDG*) causes neuroblast overproliferation in larval CNS. A constitutively active Notch receptor derivative (Notch$^{\Delta E}$) was overexpressed in the neuroblasts and GMCs under the *grh-Gal4* driver. A. Supernumerary neuroblasts (Dpn positive cells) arise both in the central brain and in the VNC as opposed to the wild-type (left panel) in which they arise as individuals. B. *D. melanogaster* genetic scheme for CNS hyperplasia generation.

3.4. Tumor transcriptome profiling.

Aberrant Notch signaling may result in a robust hyperplastic phenotype of the affected tissue and, under certain conditions, in tumor formation (Ntziachristos *et al.*, 2014). In the established scheme (see section 2.2.1), we "favored" the NB state, at the expense of the larval neurogenesis, generating hypeplastic CNSs so as to put in context the upcoming malignancy potential.

In an attempt to decipher the neoplasia generation dynamics of such CNSs, we introduced the following hypothesis: several Notch-regulated ectopically expressed factors serve the transition from the hyperplastic to the neoplastic state. To address this hypothesis, we suggested an RNA-seq analysis so as to specify the transcriptomic signature of the outgrown tumor tissue of defined genotypic origin along with tumor temporal progression. The RNA-seq comparison analysis included two temporally distinct allograft passages (T_0 versus T_3) (see section 2.3).

We intentionally selected T_0 and T_3 passages for RNA-seq analysis in order to safely address (i) whether there are certain undifferentiation markers that get "switched-off" along with cancer progression, (ii) whether the expression of certain known oncogenes/ tumor suppresors alters along with cancer progression, and finally (iii) the expression of potent novel markers indicative of cancer spatiotemporal progression.

As previously described (see sections 2.2.1, 2.3), tumor tissue of the first allograft passage (T_0) of both *hsFLP; UAS-Notch$^{\Delta E}$/ +; act5C-FRT-stop-FRT-Gal4 UAS-nlsEGFP / +* and *hsFLP; UAS-E(spl)mγ UAS-Dpn/ +; act5C-FRT-stop-FRT-Gal4 UAS-nlsEGFP / +* genotypes has been harvested and stored; sufficient for two RNA-seq biological replicates each. The tumor tissue collection of the fourth allograft passage (third re-transplantation, or T_3) followed by the RNA-seq analysis are still in progress.

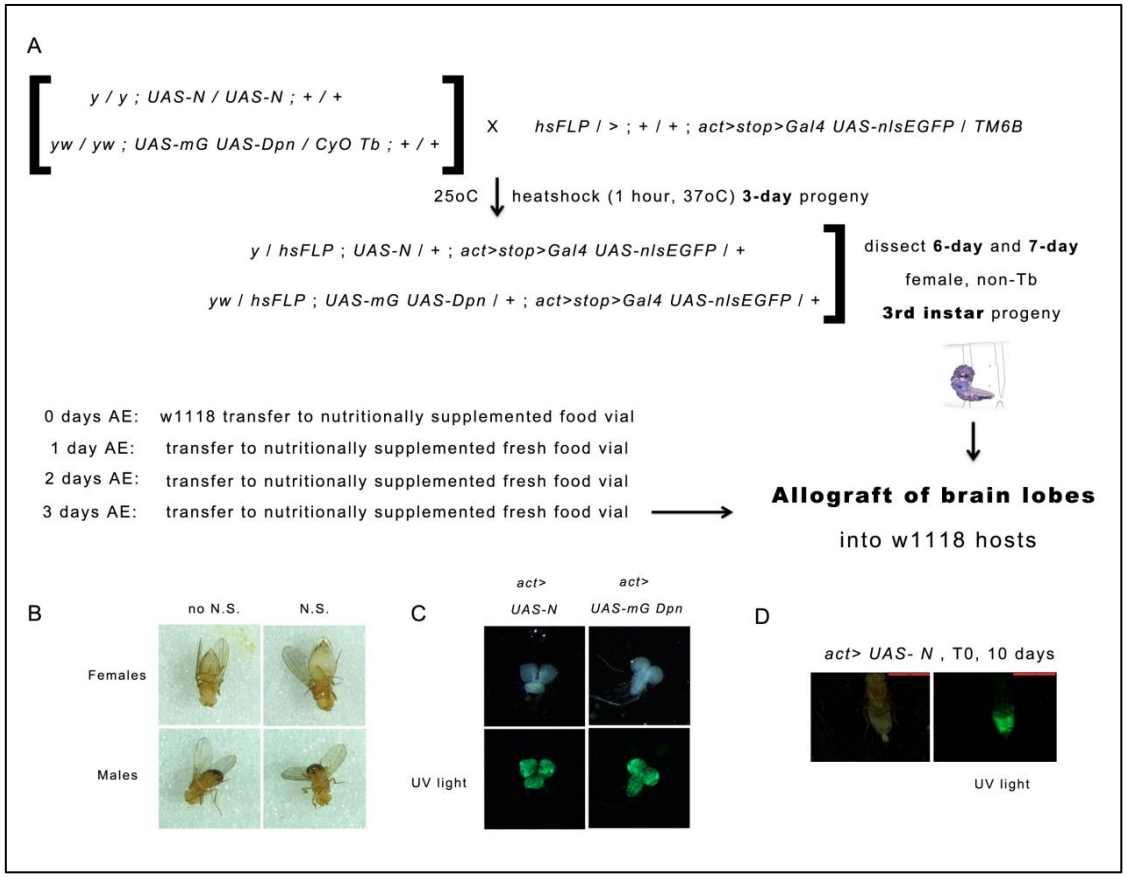

Figure 7. Hyperplastic central nervous system generation and allograft assay workflow. A. *D. melanogaster* genetics for hyperplastic CNS generation, nutritional preparation of w^{1118} host flies to be allografted. B. Nutritionally supplemented female and male individuals, out of which solely the females get allografted. Note the increase in female abromen size upon nutritional supplementation, which facilitates tumor transplantation. C. GFP positive primary hyperplastic CNSs of both $Notch^{\Delta E}$ and $E(spl)m^{\gamma}$ *Dpn* origin. D. Tumor outgrowth monitoring. N.S.: nutritionally supplemented, AE: After eclosion.

3.5. Allograft histology analysis.

Hyperplastic to neoplastic transition needs to be studied not only in terms of the transcriptome signature (see section 3.4), but also in histological terms (e.g. undifferentiation/ differentiation markers expression, differentiation potential). Published work strongly argues in favor of tumor cell infiltration within healthy tissues and metastatic foci development in wild-type hosts (driven by either *lgl*- or *brat*-deficient genetic background) (Beaucher *et al.*, 2007).

In this context, we asked the extent (if any) that the $Notch^{\Delta E}$- and double *HES*-overexpressing *E(spl)mγ Dpn*-derived tumors provoke infiltration of tumor cells within the healthy tissues. Additionally, we asked the extent (if any) that the tumor tissue undergoes any gradual differentiation (upon allografting) and whether such differentiation is genotype-dependent.

We performed immunohistochemistry analysis of tumor tissue of *hsFLP; UAS-E(spl)mγ UAS-Dpn/ +; act5C-FRT-stop-FRT-Gal4 UAS-nlsEGFP /* + origin from T_0 nls-EGFP positive allograft individuals. We mounted separately midgut epithelia, ovarian epithelia as well as carcass (Figure 8) and screened for *nls-EGFP*-expressing cells within healthy tissues. Although tumor tissue was seen adhering to the outside of adult organs, we did not observe any infiltration of tumor cells inside the protective muscle peritoneal sheaths of either ovary or gut. However, we are in need of wider infiltration screening in both genotype-wise and in temporal-wise manner (screen for infiltration in a wider range of allograft passages).

To test for possible differentiation of tumor cells, we performed immunohistochemistry analysis of mounted tumor tissue (derived by the aforementioned genotypes) and screened for *Elav*-expressing cells, within the *nls-EGFP*-expressing clones. Elav is an RNA-binding protein expressed specifically in neurons. We detected the presence of a small number of *Elav*-expressing cells within tumor tissue, indicating neuronal differentiation within the tumor clone (both *nlsEGFP*- and *Elav*-expressing cells) (Figure 7). We, however, still miss comparative analysis of temporal dynamics of differentiation potential across several passages.

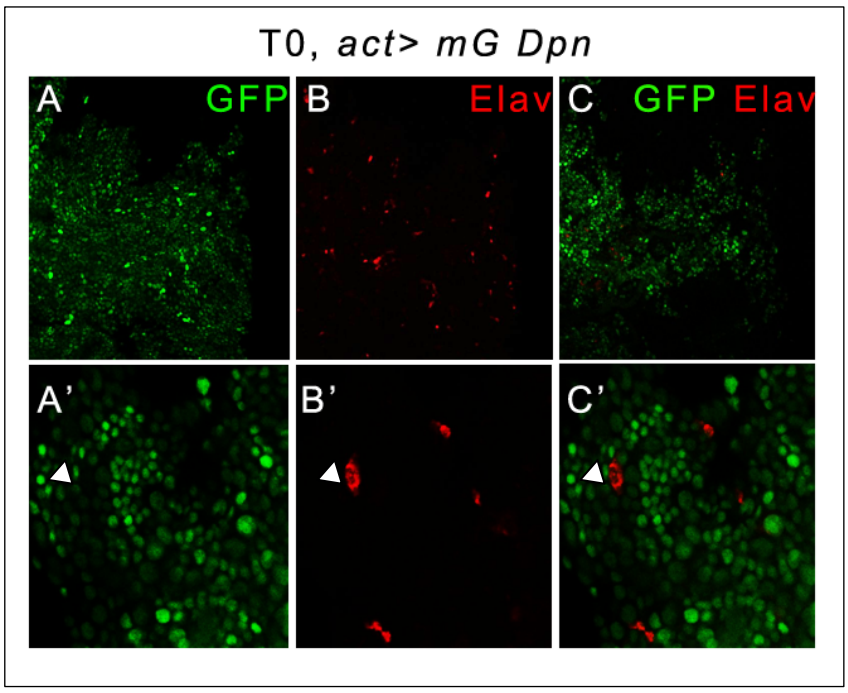

Figure 7. Undifferentiated cell state within tumor clones shows limited differentiation capacity towards the neuronal state. The majority of *nlsEGFP*-expressing cells (tumor cells) (A, A') do not express terminal differentiation markers (e.g Elav) (B, B'). However, distinct cells within the tumor clones express *Elav* (B, B', C, C') suggesting that these cells have acquired a terminally differentiated identity (arrowhead).

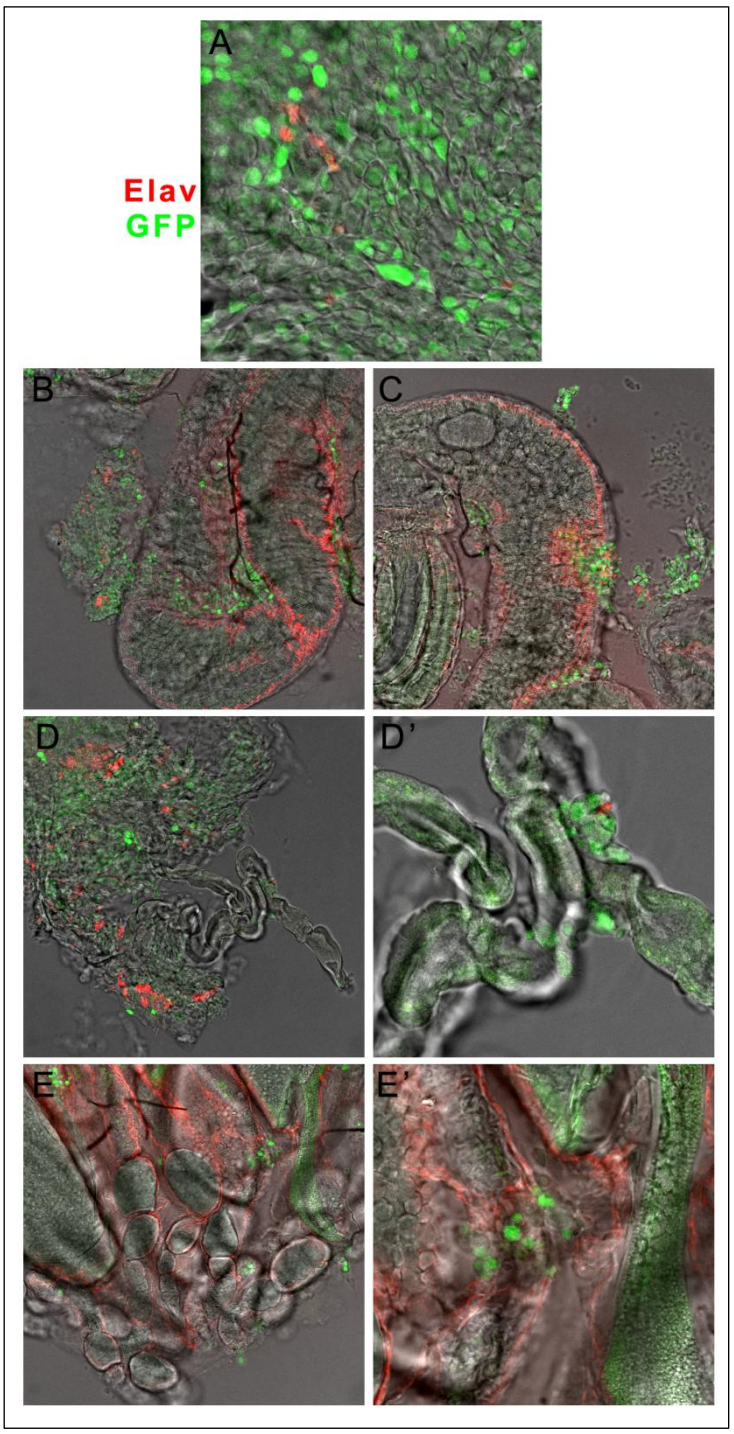

Figure 8. The double *HES*-overexpressing *E(spl)m$^{\gamma}$ Dpn*-derived tumors do not provoke infiltration of tumor cells within the healthy tissues during the first allograft passage (T_0). In detail, the histology of T_0 *E(spl)m$^{\gamma}$ Dpn*-allografted individuals has been screened for infiltrating tumor cells (nlsEGFP-positive) within midgut (B, C), trachea (D, D') and ovarian epithelia (E, E'). Note that the Elav-positive cells are suggest the presence of terminally differentiated neuronal cells. Tumor specimens have been separately immunostained (α-Elav) and screened for nlsEGFP-positive cells (A).

4. Discussion.

In our studies we aim to examine the role of Notch pathway in tumorigenesis. We seek to unveil how Notch-imposed fate-decisions break the developmental homeostasis, leading to carcinogenesis, tumor progression and cancer cell survival.

During the development of *D. melanogaster* CNS, Notch signaling is highly implicated in the cell-fate determination context via regulating of the NBs' asymmetric cell division (Muskavitch, 1994; Lai, 2004; Campos-Ortega and Knust, 1990). *UAS-Gal4*-mediated Notch hyperactivation in the NBs and their immediate progeny (GMCs) is sufficient to result in hyperplastic CNSs capable of generating malignant tumors (Zacharioudaki *et al.*, 2012; Zacharioudaki *et al.*, 2016; Magadi *et al.*, in preparation). This finding is in agreement with the oncogenic state of mammalian Notch homologues in several hematopoietic and solid tumor contexts (Ntziachristos *et al.*, 2014; Lobry *et al.*, 2011; Lobry *et al.*, 2014).

In order to investigate the molecular and cellular basis of tumor outgrowth and specify the differentially expressed genes that may take part in a tumor-forming/ tumor-maintaining network, we are conducting a tumor tissue transcriptome analysis. We plan to identify the gene groups that, once perturbed, result in more aggressive tumor derivatives. After characterization of such gene markers (possibly regulators of e.g. cell cycle, cell division, apoptosis, cell adhesion, signal transducers, lncRNAs), we plan to establish genetic schemes for *in vivo* validation.

Furthermore, the outgrowing tumor cells within allografted individuals take advantage of the *Drosophila*'s open circulatory system migrating towards several epithelial tissues (Figure 8). Tumor cell migration could result in infiltration events within healthy tissues and putatively metastases' initiation (Hanahan and Weinberg, 2000; Hanahan and Weinberg, 2011). As such, the epithelial tissues proximal to the injection spot (abdominal spot) (e.g. intestinal epithelium, ovarian epithelium), as well as distal epithelia (e.g. eye epithelium) remain to be monitored for tumor infiltration events.

The developing three-component genetic "tool" (*UAS-NPDG*, *grh-Gal4*, *hsFLP*) aims to study the tumor reversion capacity (if any) upon removal of the Notch hyperactivity. Finally, the tumor tissue that lacks the tumorigenic "trigger" $Notch^{\Delta E}$ may be compared in terms of transcriptome to constant $Notch^{\Delta E}$ active tumor tissue.

5. References.

Adam JC, Pringle JR, Peifer M. **Evidence for functional differentiation among *Drosophila* septins in cytokinesis and cellularization.** Mol Biol Cell. 2000 Sep;11(9):3123-35.

Akong K, Grevengoed EE, Price MH, McCartney BM, Hayden MA, DeNofrio JC, Peifer M. ***Drosophila* APC2 and APC1 play overlapping roles in wingless signaling in the embryo and imaginal discs.** Dev Biol. 2002 Oct 1;250 (1):91-100.

Akong K, McCartney BM, Peifer M. ***Drosophila* APC2 and APC1 have overlapping roles in the larval brain despite their distinct intracellular localizations.** Dev Biol. 2002 Oct 1;250(1):71-90.

Ambegaokar SS, Jackson GR. **Interaction between eye pigment genes and tau-induced neurodegeneration in *Drosophila melanogaster*.** Genetics. 2010 Sep;186(1):435-42.

Barolo S, Stone T, Bang AG, Posakony JW. **Default repression and Notch signaling: Hairless acts as an adaptor to recruit the corepressors Groucho and dCtBP to Suppressor of Hairless.** Genes Dev. 2002 Aug 1;16(15):1964-76.

Bayraktar OA, Boone JQ, Drummond ML, Doe CQ. **Drosophila type II neuroblast lineages keep Prospero levels low to generate large clones that contribute to the adult brain central complex.** Neural Dev. 2010 Oct 1;5:26.

Beaucher M, Goodliffe J, Hersperger E, Trunova S, Frydman H, Shearn A. ***Drosophila* brain tumor metastases express both neuronal and glial cell type markers.** Dev Biol. 2007 Jan 1;301(1):287-97.

Beaucher M, Hersperger E, Page-McCaw A, Shearn A. **Metastatic ability of *Drosophila* tumors depends on MMP activity.** Dev Biol. 2007 Mar 15;303(2):625-34.

Bello B, Reichert H, Hirth F. **The brain tumor gene negatively regulates neural progenitor cell proliferation in the larval central brain of *Drosophila*.** Development. 2006 Jul;133(14):2639-48.

Berger C, Harzer H, Burkard TR, Steinmann J, van der Horst S, Laurenson AS, Novatchkova M, Reichert H, Knoblich JA. **FACS purification and transcriptome analysis of *Drosophila* neural stem cells reveals a role for Klumpfuss in self-renewal.** Cell Rep. 2012 Aug 30;2(2):407-18.

Betschinger J, Mechtler K, Knoblich JA. **Asymmetric segregation of the tumor suppressor brat regulates self-renewal in *Drosophila* neural stem cells.** Cell. 2006 Mar 24;124(6):1241-53.

Bilder D. **Cell polarity: squaring the circle.** Curr Biol. 2001 Feb 20;11(4):R132-5. Review.

Bischof J, Maeda RK, Hediger M, Karch F, Basler K. **An optimized transgenesis system for Drosophila using germ-line-specific phiC31 integrases.** Proc Natl Acad Sci U S A. 2007 Feb 27;104(9):3312-7.

Bjornson CR, Cheung TH, Liu L, Tripathi PV, Steeper KM, Rando TA. **Notch signaling is necessary to maintain quiescence in adult muscle stem cells.** Stem Cells. 2012 Feb;30(2):232-42.

Boone JQ, Doe CQ. **Identification of Drosophila type II neuroblast lineages containing transit amplifying ganglion mother cells.** Dev Neurobiol. 2008 Aug;68(9):1185-95.

Bowman SK, Neumüller RA, Novatchkova M, Du Q, Knoblich JA. **The *Drosophila* NuMA Homolog Mud regulates spindle orientation in asymmetric cell division.** Dev Cell. 2006 Jun;10(6):731-42.

Bowman SK, Rolland V, Betschinger J, Kinsey KA, Emery G, Knoblich JA. **The tumor suppressors Brat and Numb regulate transit-amplifying neuroblast lineages in *Drosophila*.** Dev Cell. 2008 Apr;14(4):535-46.

Brody T, Odenwald WF. **Cellular diversity in the developing nervous system: a temporal view from *Drosophila*.** Development. 2002 Aug;129(16):3763-70. Review.

Cabernard C, Doe CQ. **Apical/ basal spindle orientation is required for neuroblast homeostasis and neuronal differentiation in *Drosophila***. Dev Cell. 2009 Jul;17(1):134-41.

Caldwell MC, Datta S. **Expression of cyclin E or DP/E2F rescues the G1 arrest of trol mutant neuroblasts in the *Drosophila* larval central nervous system.** Mech Dev. 1998 Dec;79(1-2):121-30.

Carthew RW. **Gene silencing by double-stranded RNA.** Curr Opin Cell Biol. 2001 Apr;13(2):244-8. Review.

Castellanos E, Dominguez P, Gonzalez C. **Centrosome dysfunction in *Drosophila* neural stem cells causes tumors that are not due to genome instability.** Curr Biol. 2008 Aug 26;18(16):1209-14.

Caussinus E, Gonzalez C. **Induction of tumor growth by altered stem-cell asymmetric division in Drosophila melanogaster.** Nat Genet. 2005 Oct;37(10):1125-9.

Ceron J, González C, Tejedor FJ. **Patterns of cell division and expression of asymmetric cell fate determinants in postembryonic neuroblast lineages of *Drosophila*.** Dev Biol. 2001 Feb 15;230(2):125-38.

Chell JM, Brand AH. **Nutrition-responsive glia control exit of neural stem cells from quiescence.** Cell. 2010 Dec 23;143(7):1161-73.

Chen HJ, Wang CM, Wang TW, Liaw GJ, Hsu TH, Lin TH, Yu JY. **The Hippo pathway controls polar cell fate through Notch signaling during *Drosophila* oogenesis.** Dev Biol. 2011 Sep 15;357(2):370-9.

Chitnis A, Henrique D, Lewis J, Ish-Horowicz D, Kintner C. **Primary neurogenesis in *Xenopus* embryos regulated by a homologue of the *Drosophila* neurogenic gene *Delta*.** Nature. 1995 Jun 29;375(6534):761-6.

Cordle J, Johnson S, Tay JZ, Roversi P, Wilkin MB, de Madrid BH, Shimizu H, Jensen S, Whiteman P, Jin B, Redfield C, Baron M, Lea SM, Handford PA. **A conserved face of the Jagged/Serrate DSL domain is involved in Notch trans-activation and cis-inhibition.** Nat Struct Mol Biol. 2008 Aug;15(8):849-57.

Datta S. **Control of proliferation activation in quiescent neuroblasts of the *Drosophila* central nervous system.** Development. 1995 Apr;121(4):1173-82.

Doe CQ. **Cell polarity: the PARty expands.** Nat Cell Biol. 2001 Jan;3(1):E7-9. Review.

Doe CQ. **Neural stem cells: balancing self-renewal with differentiation.** Development. 2008 May;135(9):1575-87.

Dumstrei K, Wang F, Hartenstein V**. Role of DE-cadherin in neuroblast proliferation, neural morphogenesis, and axon tract formation in *Drosophila* larval brain development.** J Neurosci. 2003 Apr 15;23(8):3325-35.

Dumstrei K, Wang F, Nassif C, Hartenstein V. **Early development of the *Drosophila* brain: V. Pattern of postembryonic neuronal lineages expressing DE-cadherin.** J Comp Neurol. 2003 Jan 20;455(4):451-62.

Eliasz S, Liang S, Chen Y, De Marco MA, Machek O, Skucha S, Miele L, Bocchetta M. **Notch-1 stimulates survival of lung adenocarcinoma cells during hypoxia by activating the IGF-1R pathway.** Oncogene. 2010 Apr 29;29(17):2488-98.

Fish MP, Groth AC, Calos MP, Nusse R. **Creating transgenic *Drosophila* by microinjecting the site-specific *phiC31* integrase mRNA and a transgene-containing donor plasmid.** Nat Protoc. 2007;2(10):2325-31.

Fryer CJ, Lamar E, Turbachova I, Kintner C, Jones KA. **Mastermind mediates chromatin-specific transcription and turnover of the Notch enhancer complex.** Genes Dev. 2002 Jun 1;16(11):1397-411.

Fryer CJ, White JB, Jones KA. **Mastermind recruits CycC:CDK8 to phosphorylate the Notch ICD and coordinate activation with turnover.** Mol Cell. 2004 Nov 19;16(4):509-20.

Fuerstenberg S, Giniger E. **Multiple roles for notch in *Drosophila* myogenesis.** Dev Biol. 1998 Sep 1;201(1):66-77.

Furriols M, Bray S. **A model Notch response element detects Suppressor of Hairless-dependent molecular switch.** Curr Biol. 2001 Jan 9;11(1):60-4.

Gateff E. **Tumor suppressor and overgrowth suppressor genes of Drosophila melanogaster: developmental aspects.** Int J Dev Biol. 1994 Dec;38(4):565-90.

Groth AC, Fish M, Nusse R, Calos MP. **Construction of transgenic *Drosophila* by using the site-specific integrase from phage *phiC31*.** Genetics. 2004 Apr;166(4):1775-82.

Haines N, Irvine KD. **Glycosylation regulates Notch signalling.** Nat Rev Mol Cell Biol. 2003 Oct;4(10):786-97. Review.

Handler AM, Harrell RA 2nd. **Germline transformation of *Drosophila melanogaster* with the piggyBac transposon vector.** Insect Mol Biol. 1999 Nov;8(4):449-57.

Hubbard EJ, Wu G, Kitajewski J, Greenwald I. **sel-10, a negative regulator of lin-12 activity in *Caenorhabditis elegans*, encodes a member of the CDC4 family of proteins.** Genes Dev. 1997 Dec 1;11(23):3182-93.

Ito K, Hotta Y. **Proliferation pattern of postembryonic neuroblasts in the brain of *Drosophila melanogaster*.** Dev Biol. 1992 Jan;149(1):134-48.

Izumi Y, Ohta N, Hisata K, Raabe T, Matsuzaki F. ***Drosophila* Pins-binding protein Mud regulates spindle-polarity coupling and centrosome organization.** Nat Cell Biol. 2006 Jun;8(6):586-93.

Jarriault S, Le Bail O, Hirsinger E, Pourquié O, Logeat F, Strong CF, Brou C, Seidah NG, Isra l A. **Delta-1 activation of notch-1 signaling results in HES-1 transactivation.** Mol Cell Biol. 1998 Dec;18(12):7423-31.

Kao HY, Ordentlich P, Koyano-Nakagawa N, Tang Z, Downes M, Kintner CR, Evans RM, Kadesch T. **A histone deacetylase corepressor complex regulates the Notch signal transduction pathway.** Genes Dev. 1998 Aug 1;12(15):2269-77.

Klinakis A, Lobry C, Abdel-Wahab O, Oh P, Haeno H, Buonamici S, van De Walle I, Cathelin S, Trimarchi T, Araldi E, Liu C, Ibrahim S, Beran M, Zavadil J, Efstratiadis A, Taghon T, Michor F, Levine RL, Aifantis I. **A novel tumour-suppressor function for the Notch pathway in myeloid leukaemia.** Nature. 2011 May 12;473(7346):230-3.

Knoblich JA. **Mechanisms of asymmetric stem cell division.** Cell. 2008 Feb 22;132(4):583-97.

Knoblich JA. **Neurobiology: getting axons going.** Nature. 2005 Aug 4;436(7051):632-3.

Kopan R, Ilagan MX. **The canonical Notch signaling pathway: unfolding the activation mechanism.** Cell. 2009 Apr 17;137(2):216-33.

Kopan R, Nye JS, Weintraub H. **The intracellular domain of mouse Notch: a constitutively activated repressor of myogenesis directed at the basic helix-loop-helix region of MyoD.** Development. 1994 Sep;120(9):2385-96.

Kovall RA, Blacklow SC. **Mechanistic insights into Notch receptor signaling from structural and biochemical studies.** Curr Top Dev Biol. 2010;92:31-71.

Kraut R, Campos-Ortega JA. **inscuteable, a neural precursor gene of Drosophila, encodes a candidate for a cytoskeleton adaptor protein.**Dev Biol. 1996 Feb 25;174(1):65-81.

Kurooka H, Honjo T. **Functional interaction between the mouse *notch1* intracellular region and histone acetyltransferases PCAF and GCN5.** J Biol Chem. 2000 Jun 2;275(22):17211-20.

Lai EC. **Notch signaling: control of cell communication and cell fate.** Development. 2004 Mar;131(5):965-73. Review.

Lamar E, Kintner C, Goulding M. **Identification of NKL, a novel Gli-Kruppel zinc-finger protein that promotes neuronal differentiation.** Development. 2001 Apr;128(8):1335-46.

Lee CY, Andersen RO, Cabernard C, Manning L, Tran KD, Lanskey MJ, Bashirullah A, Doe CQ. ***Drosophila* Aurora-A kinase inhibits neuroblast self-renewal by regulating aPKC/Numb cortical polarity and spindle orientation.** Genes Dev. 2006 Dec 15;20(24):3464-74.

Lei L, Xu A, Panin VM, Irvine KD. **An O-fucose site in the ligand binding domain inhibits Notch activation.** Development. 2003 Dec;130(26):6411-21.

Lobry C, Oh P, Aifantis I. **Oncogenic and tumor suppressor functions of Notch in cancer: it's NOTCH what you think.** J Exp Med. 2011 Sep 26;208(10):1931-5.

Lobry C, Oh P, Mansour MR, Look AT, Aifantis I. **Notch signaling: switching an oncogene to a tumor suppressor.** Blood. 2014 Apr 17;123(16):2451-9.

Lu B, Rothenberg M, Jan LY, Jan YN. **Partner of Numb colocalizes with Numb during mitosis and directs Numb asymmetric localization in Drosophila neural and muscle progenitors.** Cell. 1998 Oct 16;95(2):225-35.

Luca VC, Jude KM, Pierce NW, Nachury MV, Fischer S, Garcia KC. **Structural biology. Structural basis for Notch1 engagement of Delta-like 4.** Science. 2015 Feb 20;347(6224):847-53.

Manseau L, Baradaran A, Brower D, Budhu A, Elefant F, Phan H, Philp AV, Yang M, Glover D, Kaiser K, Palter K, Selleck S. **GAL4 enhancer traps expressed in the embryo, larval brain, imaginal discs, and ovary of *Drosophila***. Dev Dyn. 1997 Jul;209(3):310-22.

Markstein M, Pitsouli C, Villalta C, Celniker SE, Perrimon N. **Exploiting position effects and the gypsy retrovirus insulator to engineer precisely expressed transgenes.** Nat Genet. 2008 Apr;40(4):476-83.

Matthews KA, Kaufman TC, Gelbart WM. **Research resources for *Drosophila*: the expanding universe.** Nat Rev Genet. 2005 Mar;6(3):179-93. Review.

Maurange C, Gould AP. **Brainy but not too brainy: starting and stopping neuroblast divisions in *Drosophila*.** Trends Neurosci. 2005 Jan;28(1):30-6.

Morel V, Lecourtois M, Massiani O, Maier D, Preiss A, Schweisguth F. **Transcriptional repression by suppressor of hairless involves the binding of a hairless-dCtBP complex in *Drosophila*.** Curr Biol. 2001 May 15;11(10):789-92.

Morel V, Schweisguth F. **Repression by suppressor of hairless and activation by Notch are required to define a single row of single-minded expressing cells in the *Drosophila* embryo.** Genes Dev. 2000 Feb 1;14(3):377-88.

Mourikis P, Gopalakrishnan S, Sambasivan R, Tajbakhsh S. **Cell-autonomous Notch activity maintains the temporal specification potential of skeletal muscle stem cells.** Development. 2012 Dec;139(24):4536-48.

Muskavitch MA. **Delta-notch signaling and *Drosophila* cell fate choice.** Dev Biol. 1994 Dec;166(2):415-30.

Nakao K, Campos-Ortega JA. **Persistent expression of genes of the enhancer of split complex suppresses neural development in *Drosophila*.** Neuron. 1996 Feb;16(2):275-86.

Nam Y, Sliz P, Song L, Aster JC, Blacklow SC. **Structural basis for cooperativity in recruitment of MAML coactivators to Notch transcription complexes.** Cell. 2006 Mar 10;124(5):973-83.

Neumüller RA, Knoblich JA. **Dividing cellular asymmetry: asymmetric cell division and its implications for stem cells and cancer.** Genes Dev. 2009 Dec 1;23(23):2675-99.

Niessen K, Fu Y, Chang L, Hoodless PA, McFadden D, Karsan A. **Slug is a direct Notch target required for initiation of cardiac cushion cellularization.** J Cell Biol. 2008 Jul 28;182(2):315-25.

Ntziachristos P, Lim JS, Sage J, Aifantis I. **From fly wings to targeted cancer therapies: a centennial for notch signaling.** Cancer Cell. 2014 Mar 17;25(3):318-34.

O'Connor M, Chia W. **P element-mediated germ-line transformation of *Drosophila*.** Methods Mol Biol. 1993;18:75-85.

Ohno S. **Intercellular junctions and cellular polarity: the PAR-aPKC complex, a conserved core cassette playing fundamental roles in cell polarity.** Curr Opin Cell Biol. 2001 Oct;13(5):641-8.

Okajima T, Xu A, Irvine KD. **Modulation of notch-ligand binding by protein O-fucosyltransferase 1 and fringe.** J Biol Chem. 2003 Oct 24;278(43):42340-5.

Palomero T, Lim WK, Odom DT, Sulis ML, Real PJ, Margolin A, Barnes KC, O'Neil J, Neuberg D, Weng AP, Aster JC, Sigaux F, Soulier J, Look AT, Young RA, Califano A, Ferrando AA. **NOTCH1 directly regulates c-MYC and activates a feed-forward-loop transcriptional network promoting leukemic cell growth.** Proc Natl Acad Sci U S A. 2006 Nov 28;103(48):18261-6.

Park Y, Rangel C, Reynolds MM, Caldwell MC, Johns M, Nayak M, Welsh CJ, McDermott S, Datta S. ***Drosophila*** **perlecan modulates FGF and hedgehog signals to activate neural stem cell division.** Dev Biol. 2003 Jan 15;253(2):247-57.

Parks AL, Huppert SS, Muskavitch MA. **The dynamics of neurogenic signalling underlying bristle development in *Drosophila melanogaster*.** Mech Dev. 1997 Apr;63(1):61-74.

Pearson J, López-Onieva L, Rojas-Ríos P, González-Reyes A. **Recent advances in *Drosophila* stem cell biology.** Int J Dev Biol. 2009;53(8-10):1329-39.

Prokop A, Bray S, Harrison E, Technau GM. **Homeotic regulation of segment-specific differences in neuroblast numbers and proliferation in the *Drosophila* central nervous system.** Mech Dev. 1998 Jun;74(1-2):99-110.

Ramain P, Khechumian K, Seugnet L, Arbogast N, Ackermann C, Heitzler P. **Novel *Notch* alleles reveal a Deltex-dependent pathway repressing neural fate.** Curr Biol. 2001 Nov 13;11(22):1729-38.
Rangarajan A, Talora C, Okuyama R, Nicolas M, Mammucari C, Oh H, Aster JC, Krishna S, Metzger D, Chambon P, Miele L, Aguet M, Radtke F, Dotto GP. **Notch signaling is a direct determinant of keratinocyte growth arrest and entry into differentiation.** EMBO J. 2001 Jul 2;20(13):3427-36.

Reizis B, Leder P. **Direct induction of T lymphocyte-specific gene expression by the mammalian Notch signaling pathway.** Genes Dev. 2002 Feb 1;16(3):295-300.

Rolls MM, Albertson R, Shih HP, Lee CY, Doe CQ. ***Drosophila*** **aPKC regulates cell polarity and cell proliferation in neuroblasts and epithelia.** J Cell Biol. 2003 Dec 8;163(5):1089-98.

Ronchini C, Capobianco AJ. **Induction of cyclin D1 transcription and CDK2 activity by Notch(ic): implication for cell cycle disruption in transformation by Notch(ic).** Mol Cell Biol. 2001 Sep;21(17):5925-34.

Rossi F, Gonzalez C. **Studying tumor growth in *Drosophila* using the tissue allograft method.** Nat Protoc. 2015 Oct;10(10):1525-34.

Rubin GM, Spradling AC. **Vectors for P element-mediated gene transfer in *Drosophila*.** Nucleic Acids Res. 1983 Sep 24;11(18):6341-51.

San-Juán BP, Baonza A. **The bHLH factor deadpan is a direct target of Notch signaling and regulates neuroblast self-renewal in *Drosophila*.** Dev Biol. 2011 Apr 1;352(1):70-82.

Schaefer M, Shevchenko A, Shevchenko A, Knoblich JA. A protein complex containing **Inscuteable** and the Galpha-binding protein Pins orients asymmetric cell divisions in Drosophila. Curr Biol. 2000 Apr 6;10(7):353-62.

Schober M, Schaefer M, Knoblich JA. **Bazooka recruits Inscuteable to orient asymmetric cell divisions in *Drosophila* neuroblasts.** Nature. 1999 Dec 2;402(6761):548-51.

Siller KH, Cabernard C, Doe CQ. **The NuMA-related Mud protein binds Pins and regulates spindle orientation in *Drosophila* neuroblasts.** Nat Cell Biol. 2006 Jun;8(6):594-600.

Sonoda J, Wharton RP. ***Drosophila* Brain Tumor is a translational repressor.** Genes Dev. 2001 Mar 15;15(6):762-73.

Sousa-Nunes R, Yee LL, Gould AP. **Fat cells reactivate quiescent neuroblasts via TOR and glial insulin relays in Drosophila.** Nature. 2011 Mar 24;471(7339):508-12.

Spana EP, Doe CQ. **The prospero transcription factor is asymmetrically localized to the cell cortex during neuroblast mitosis in *Drosophila*.** Development. 1995 Oct;121(10):3187-95.

Suzuki A, Ohno S. **The PAR-aPKC system: lessons in polarity.** J Cell Sci. 2006 Mar 15;119(Pt 6):979-87. Review.

Trimarchi T, Bilal E, Ntziachristos P, Fabbri G, Dalla-Favera R, Tsirigos A, Aifantis I. **Genome-wide mapping and characterization of Notch-regulated long noncoding RNAs in acute leukemia.** Cell. 2014 Jul 31;158(3):593-606.

Tweedie S, Ashburner M, Falls K, Leyland P, McQuilton P, Marygold S, Millburn G, Osumi-Sutherland D, Schroeder A, Seal R, Zhang H; FlyBase Consortium. **FlyBase: enhancing Drosophila Gene Ontology annotations.** Nucleic Acids Res. 2009 Jan;37 (Database issue):D555-9.

Urbach R, Schnabel R, Technau GM. **The pattern of neuroblast formation, mitotic domains and proneural gene expression during early brain development in *Drosophila*.** Development. 2003 Aug;130(16):3589-606.

van Tetering G, van Diest P, Verlaan I, van der Wall E, Kopan R, Vooijs M. **Metalloprotease ADAM10 is required for Notch1 site 2 cleavage.** J Biol Chem. 2009 Nov 6;284(45):31018-27.

Vasyutina E, Lenhard DC, Birchmeier C. **Notch function in myogenesis.** Cell Cycle. 2007 Jun 15;6(12):1451-4.

Vilimas T, Mascarenhas J, Palomero T, Mandal M, Buonamici S, Meng F, Thompson B, Spaulding C, Macaroun S, Alegre ML, Kee BL, Ferrando A, Miele L, Aifantis I. **Targeting the NF-kappaB signaling pathway in Notch1-induced T-cell leukemia.** Nat Med. 2007 Jan;13(1):70-7.

Wallberg AE, Pedersen K, Lendahl U, Roeder RG. **p300 and PCAF act cooperatively to mediate transcriptional activation from chromatin templates by notch intracellular domains in vitro.** Mol Cell Biol. 2002 Nov;22(22):7812-9.

Wang H, Ouyang Y, Somers WG, Chia W, Lu B. **Polo inhibits progenitor self-renewal and regulates Numb asymmetry by phosphorylating Pon.** Nature. 2007 Sep 6;449(7158):96-100.

Wang, W., and G. Struhl. **Distinct roles for Mind bomb, Neuralized and Epsin in mediating DSL endocytosis and signaling in *Drosophila.*** Development 2005. 132:2883–2894.

Weng AP, Millholland JM, Yashiro-Ohtani Y, Arcangeli ML, Lau A, Wai C, Del Bianco C, Rodriguez CG, Sai H, Tobias J, Li Y, Wolfe MS, Shachaf C, Felsher D, Blacklow SC, Pear WS, Aster JC. **c-Myc is an important direct target of Notch1 in T-cell acute lymphoblastic leukemia/lymphoma.** Genes Dev. 2006 Aug 1;20(15):2096-109.

Wilson JJ, Kovall RA. **Crystal structure of the CSL-Notch-Mastermind ternary complex bound to DNA.** Cell. 2006 Mar 10;124(5):985-96.

Wodarz A, Ramrath A, Kuchinke U, Knust E. **Bazooka provides an apical cue for Inscuteable localization in *Drosophila* neuroblasts.** Nature. 1999 Dec 2;402(6761):544-7.

Wu PS, Egger B, Brand AH. **Asymmetric stem cell division: lessons from *Drosophila*.** Semin Cell Dev Biol. 2008 Jun;19(3):283-93.

Xiao, Q., Komori, H. and Lee, C.-Y. **Klumpfuss distinguishes stem cells from progenitor cells during asymmetric neuroblast division.** Development(2012) 139, 2670-2680.

Younossi-Hartenstein A, Nassif C, Green P, Hartenstein V. **Early neurogenesis of the *Drosophila* brain.** J Comp Neurol. 1996 Jul 1;370(3):313-29.

Zacharioudaki E, Housden BE, Garinis G, Stojnic R, Delidakis C, Bray SJ. **Genes implicated in stem cell identity and temporal programme are directly targeted by Notch in neuroblast tumours.** Development. 2016 Jan 15;143(2):219-31.

Zacharioudaki E, Magadi SS, Delidakis C**. bHLH-O proteins are crucial for Drosophila neuroblast self-renewal and mediate Notch-induced overproliferation.** Development. 2012 Apr;139(7):1258-69.